SCIENTIFIC RESEARCH JOURNAL

Institute of Research Management and Innovation

SCIENTIFIC RESEARCH JOURNAL

Seismic Response of a Base Isolated Cable-Stayed Bridge Under Near-Fault Ground Motion Excitations

Ahad Javanmardi[1], Zainab Ibrahim, Khaled Gheadi, Mohammed Jameel, Usman Hanif, Meisam Gordan

Civil Department, Engineering Faculty, University of Malaya,
50603 Kuala Lumpur, Malaysia
[1]E-mail: ahadjavanmardi@gmail.com, ahad@siswa.um.edu.my

ABSTRACT

Nowadays, development of cable-stayed bridges is increasing around the world. The mitigation of seismic forces to these bridges are obligatory to prevent damages or failure of its structural members. Herein, this paper aimed to determine the near-fault ground motion effect on an existing cable-stayed bridge equipped with lead-rubber bearing. In this context, Shipshaw cable-stayed bridge is selected as the case study. The selected bridge has a span of 183.2 m composite deck and 43 m height of steel tower. 2D finite element models of the non-isolated and base isolated bridges are modelled by using SAP2000. Three different near-fault ground motions which are Tabas 1978, Cape Mendocino 1992 and Kobe 1995 were subjected to the 2D FEM models in order to determine the seismic behaviour of the bridge. The near-fault ground motions were applied to the bridge in the longitudinal direction. Nonlinear dynamic analysis was performed to determine the dynamic responses of the bridge. Comparison of dynamic response of non-isolated and base isolated bridge under three different near-fault ground motions were conducted. The results obtained from numerical analyses of the bridge showed that the isolation system lengthened the period of bridge and minimised deck displacement, base shear and base moment of the bridge. It is concluded that the isolation system significantly reduced the destructive effects of near-fault ground motions on the bridge.

INTRODUCTION

Ground motions or earthquake cause severe problems to the structures such as dams, bridges, buildings, infrastructures and others [1–3]. In addition, many researchers had investigated the effect of earthquakes on the structures and attempted to mitigate the destructive force of earthquake through seismic control systems [4–7]. In recent years, cable-stayed bridges are the key in transportation networks, and gained popularity due to longer span, appealing aesthetics values, economical and faster construction [6]. These bridges are associated with high flexibility, low damping and long fundamental periods [8], which make them susceptible to high amplitude oscillation under earthquake ground motions [9]. Seismic response of structures under near-fault motion are different as compare to far-field ground motion [10].

The characteristics of near-fault ground motions are: i) large long-period spectral component in normal direction of fault; ii) large-short period spectral component, parallel to fault direction; iii) high peak ground velocities and long-duration pulses of ground displacement. Seismic response of structure under near-fault ground motions significantly increase as compare to typical far-field ground motion, which are the resultant of higher spectral components in near-fault ground motions. Several studies dealt with isolation techniques of cable-stayed bridges to improve their performance under earthquake excitation [11–14].

Cable-stayed bridges are highly sensitive under large amplitude long-period ground motions, also associate with multi modes in the dynamic responses, this make the use of seismic isolation obligatory to prevent the damages under near-fault ground motions and keep the bridge in service after the earthquake [15-16].

METHODOLOGY

Shipshaw Cable-stayed Bridge

Shipshaw cable-stayed bridge used for the case study is a double-plane fan-type cable bridge. It consists of a double leg steel tower and two box girders which support a composite steel deck as shown in Figure 1. Overall length of the bridge is 183 m with four identical spans and 4% downward slope from the East to the West abutment along deck. The bridge support is founded on rock. The tower bearings are hinged and allow to rotate along their axes. The abutment bearings are roller supported to prevent the uplifting force generated by the cable forces.

The deck is 11 m wide and composed of concrete deck thickness of 165 mm with two non-structural precast parapets. In addition, the deck is supported by five longitudinal stringers spaced equally at 2.4 m interval in longitudinal direction. Floor beams transfer the stringer loads to box girders and spaced equally at 7 m interval in transverse direction. The box girder dimension is 1.5 m x 2.4 m with web and flange thickness of 50 mm. The tower is 43 m tall with two 1.5 m x 2.4 m rectangular box steel with flange and web thickness of 50 mm. Steel Grade 330 is used for box tower and box girder. Four cables are connected from each tower to the top flange of box girders. Each cable consists of nine strands with each strand cross sectional area of 65.1 mm^2. The cables have the modulus of elasticity 175 GPa, yield strength of 1500 MPa and the ultimate strength of 1725 MPa [17].
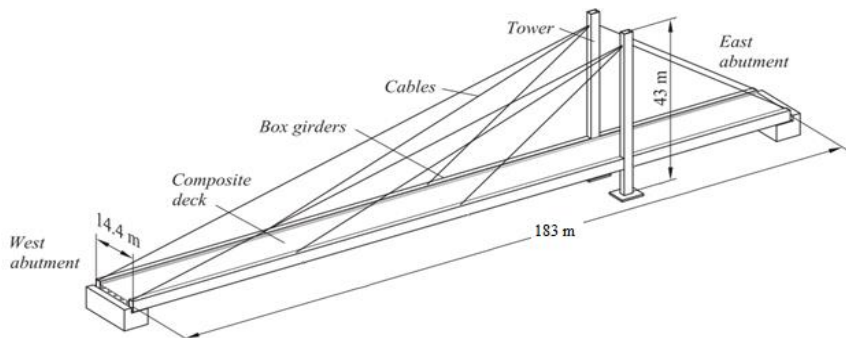
Figure 1: Detailing of Shipshaw Cable-stay Bridge

Numerical Modelling

The nonlinear dynamic response of non-isolated and isolated cable-stayed bridge subjected to longitudinal near-fault ground motions were performed in SAP2000. The bridge was modelled in two dimensions, consisted of one tower, one main box girder and four sets of cables as shown in Figure 2. Material properties used in the model are as described in previous section. The pretension forces in each cable is calculated based on the unit load method. The pretension force prevent the box girder from deflecting under its self-weight [18]. A lead rubber bearing is designed based on AASHTO specification [19-20]. The isolator device was placed at the base of pylon since the abutments are roller supporter and provide free horizontal movement of the deck. The initial stiffness of the lead rubber bearing is 15000 kN/m. The characteristics of the lead rubber bearing were input in SAP2000. Figure 3 shows the ideal force-deformation behaviour of the lead rubber bearing.
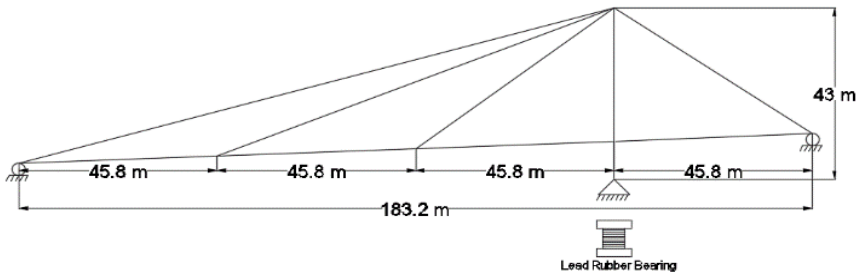
Figure 2: Bridge Model in SAP2000
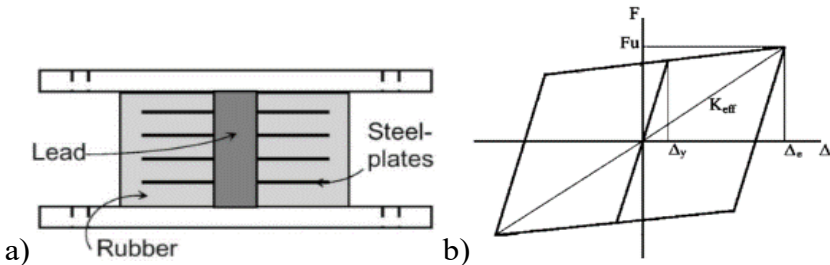
Figure 3: a) Schematic Diagrams and b) Ideal Force-Deformation Behaviour of the Lead Rubber Bearing

Near-fault Ground Motions

The seismic response of the cable-stayed bridge was studied using three near-fault ground motion records. The data and characteristics of these records are listed in Table 1 [21]. These near-fault ground motions are applied to the bridge in longitudinal direction only. A total time of ten seconds of each record was used.

Table 1: Main Characteristics of The Near-Fault Ground Motions Used in This Study [21]

No.	Earthquake name	Year	Magnitude	Distance (km)	Peak Acceleration	
					PGA (g)	Time (s)
1	Tabas	1978	7.4	1.2	0.900	10.66
2	Cape Mendocino	1992	7.1	8.5	0.655	3.60
3	Kobe	1995	6.9	3.4	0.575	4.66

NUMERICAL RESULTS AND DISCUSSION

Natural Time Period of Bridge

Table 2 shows the natural time period from the previous experimental investigation and the numerical analysis [22]. There is a reasonable agreement between three natural time periods of the longitudinal bending modes which are computed experimentally and numerically.

Table 2: Natural Time Period of Shipshaw Cable-Stay Bridge

Mode No.	Mode Type	T, Experimental (s)	T, Numerical (s)	Error (%)
1	Longitudinal bending	1.85	1.58	14.5
2	Longitudinal bnding	0.85	0.70	17.6
3	Longitudinal bending	0.57	0.43	24.5

After the implementation of the base isolator in numerical model, the natural time periods are increased significantly, as shown in Table 3. In addition, the effective modal participating mass of the first mode became 98% of the total mass of the isolated bridge which makes the first longitudinal mode as governing mode of the bridge.

Table 3: Natural Time Period of Non-Isolated and Isolated Cable-Stayed Bridge

Mode No.	Period (s)	
	Non-Isolated Bridge	Isolated Bridge
1	1.58	5.50
2	0.70	1.68
3	0.43	0.75

Deck Displacement

The maximum horizontal relative displacements of the deck for three near-fault ground motions are shown in Figure 4. The relative deck displacements are taken at the node where the box girder and the tower intersected with each other. The maximum deck displacement in non-isolated bridge is 160.56 mm under Cape Mendocino ground motion. However, after the implementation of the isolation device, it is decreased to 30.10 mm. Figure 4 indicates that the based isolator device significantly reduced the deck displacements. In addition as shown, the oscillation of the deck displacement in isolated bridge is relatively smaller than that of the non-isolated bridge, which enhances the stability of the bridge under serviceablity during earthquakes.

a) Tabas

b) Cape Mendocino
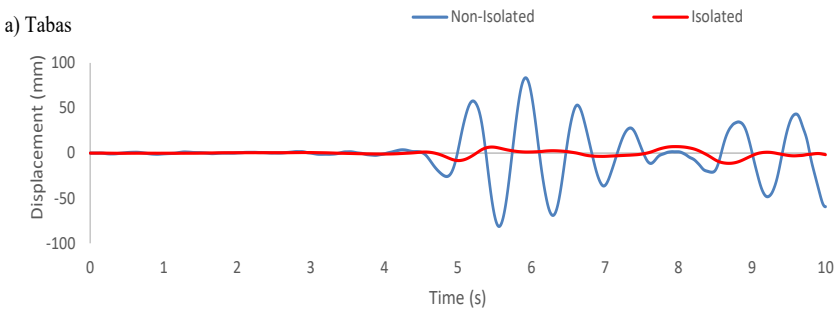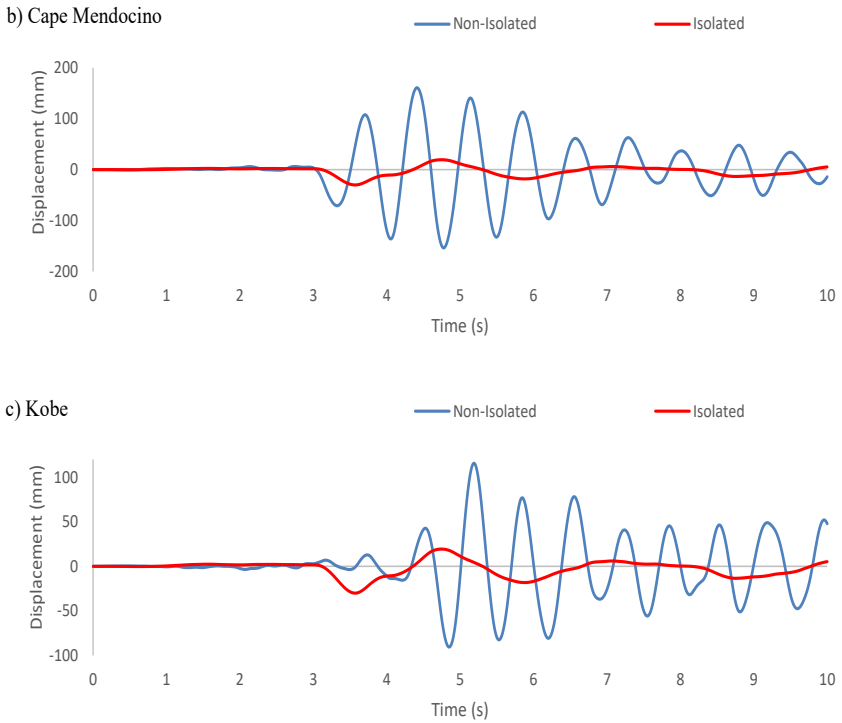
c) Kobe

Figure 4: Deck Displacements Response Due to Near-Fault Ground Motions; a) Tabas; b) Cape Mendocino and c) Kobe

Tower Base Shear

The maximum base shear was computed at the tower support as shown in Figure 5. The base shear variation over total time of each earhquake is less varying and reduced significanlty. The maximum base shear is 10983.4 kN under Cape Mendocino ground motion for non-isolated bridge and after installation of isolator device, the base shear is reduced to 1666.03 kN. As resultant, the isolator significantly decreased the base shear force of the tower.

a) Tabas

b) Cape Mendocino
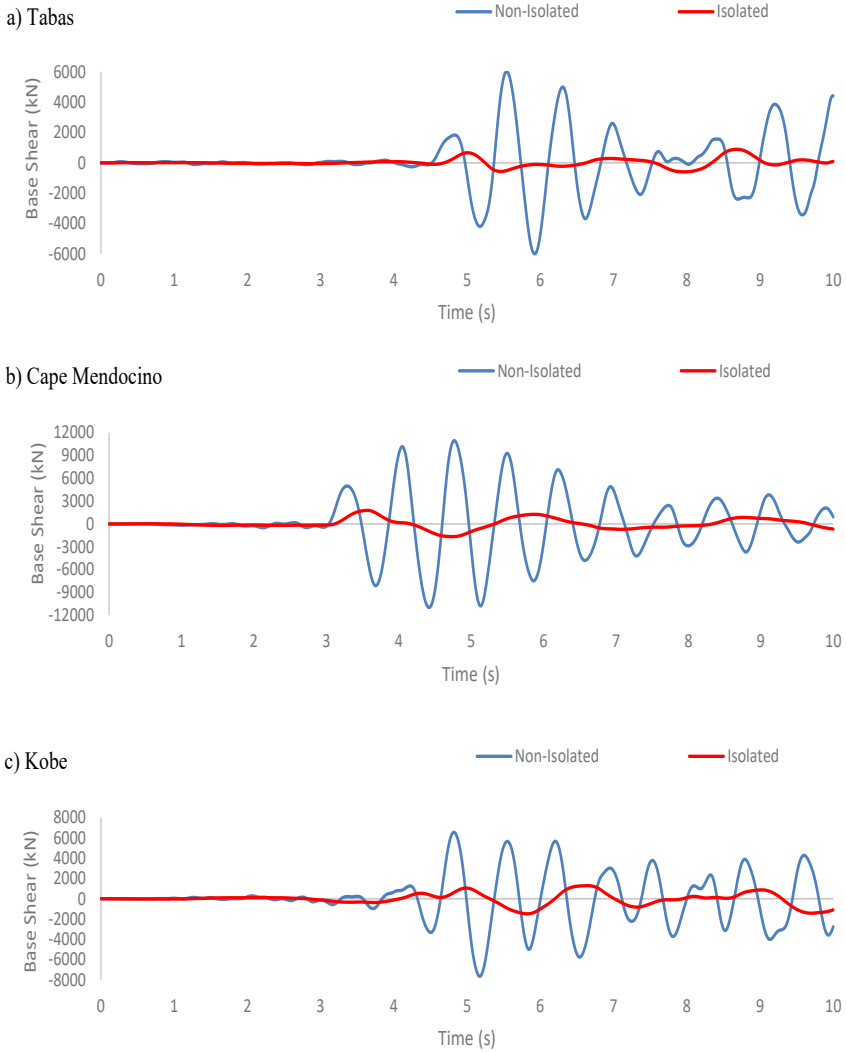
c) Kobe

Figure 5 : Tower Base Shear Response Due to Near-Fault Ground Motions; a) Tabas b) Cape Mendocino and c) Kobe

Tower Bending Moment

The maximum bending moments of the tower for three near-fault ground motions are given in Figure 6. The maximum tower bending moments are taken at the deck level. The maximum of tower bending moments of non-isolated and isolated bridge are 0.69 kNmm and 0.1017 kNmm, respectively during Cape Mendocino earthquake. As indicated in the figure, the bending moment of the tower reduced significantly under all the ground motions when the base isolation is implemented.

a) Tabas

b) Cape Mendocino
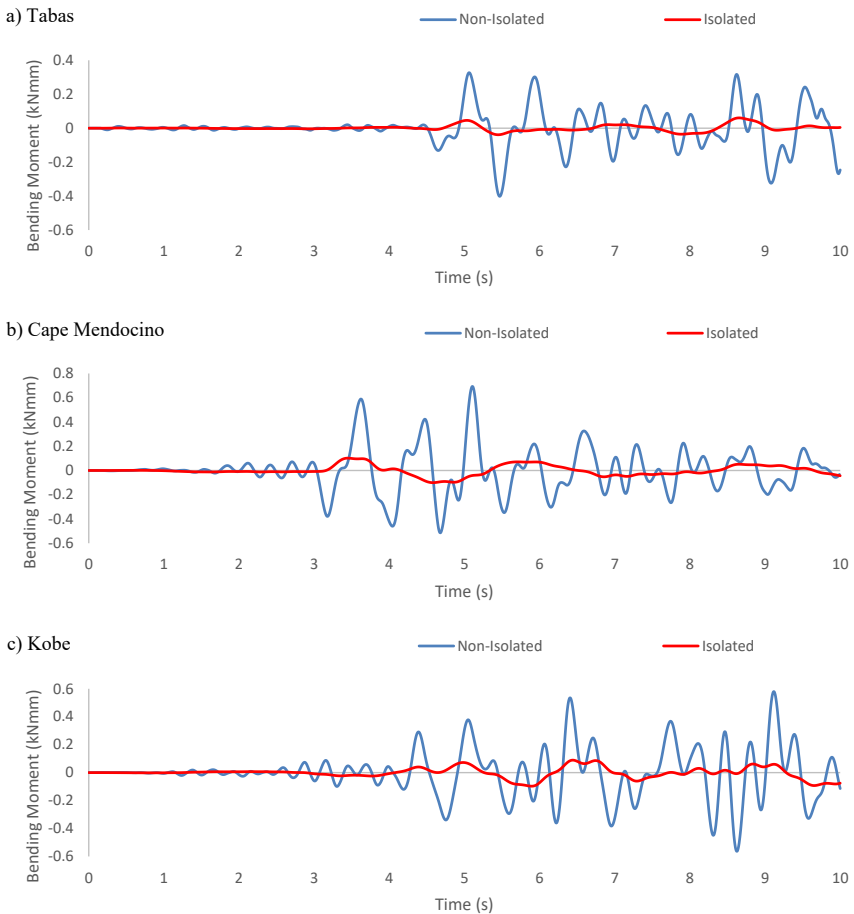
c) Kobe

Figure 6: Tower Base Bending Moment Due to Near-Fault Ground Motions; a) Tabas b) Cape Mendocino and c) Kobe

As the comparative study, the overall seismic response of the bridge is summarised in Table 4. The percentage reduction of displacements for Tabas, Cape Mendocino and Kobe earthquake ground motions are 86.40%, 81.25%, and 73.96%, respectively. In addition, the base shear reduction percentage of the tower is 85.20%, 84.83%, and 80.56%, due to Tabas, Cape Mendocino and Kobe near-fault ground motions respectively. Furthermore, the bending moment of the tower reduced by 84.89%, 85.26%, and 83.24% under Tabas, Cape Mendocino and Kobe near-fault ground motions, respectively.

Table 4: Overall Peak Responses of The Bridge Under Different Near-Fault Earthquakes

Ground Motion	Bridge Configuration	Deck Displacement (mm)	Base Shear (kN)	Base Moment (kN-mm)
Tabas	Non-isolated	83.4	6029.5	0.401
	Isolated	11.3	891.9	0.061
Cape Mendocino	Non-isolated	160.6	10983.4	0.692
	Isolated	30.1	1666.0	0.102
Kobe	Non-isolated	115.7	7641.7	0.579
	Isolated	30.1	1486.1	0.097

CONCLUSION

In general, the base isolation system of the bridge is placed below the deck. Nonetheless, in this case study, the isolator device was implemented between the tower and foundation. The isolated and non-isolated cable-stayed bridge were modeled by using SAP2000. The nonlinear dynamic response of the bridge was performed to investigate the effectiveness of the isolation system. The main conclusions of this investigation are summarised as follows:

- Implementation of the isolation device lengthened the bridge time periods, hence, decreasing the transferred acceleration and the reduction of internal forces in the bridge.

- The horizontal deck displacement, base shear and bending moment of the tower decreased significantly, after the implementation of the base isolator in cable-stayed bridge.
- The lead-rubber bearing offered some advantages for the internal force on the base isolated bridge compare to non-isolated bridge.
- The isolated bridge remained elastic under all near-fault ground motions. This abled the bridge to remain in service after strong near-fault ground motions.

ACKNOWLEDGEMENT

REFERENCES

[1] K. Ghaedi, and Z. Ibrahim, 2017. Earthquake prediction, in T. Zouaghi (Ed.), *Earthquakes - Tectonics, Hazard Risk Mitigation*, London: InTech 2017: pp. 205–227. DOI:10.5772/65511.

[2] K. Ghaedi, Z. Ibrahim, H. Adeli, and A. Javanmardi, 2017. Invited review: Recent developments in vibration control of building and bridge structures, *J. Vibroengineering, Vol. 19*(5), pp. 3564–3580. DOI:10.21595/jve.2017.18900.

[3]   A. Javanmardi, R. Abadi, A.K. Marsono, M. Tap, Z. Ibrahim, and A. Ahmad, 2014. Correlation of stiffness and natural frequency of precast frame system, *Applied Mechanics and Materials Vol. 735*, pp. 141–144. DOI: 10.4028/www.scientific.net/AMM.735.141.

[4]   K. Ghaedi, M. Jameel, Z. Ibrahim, and P. Khanzaei, 2016. Seismic analysis of roller compacted concrete (RCC) dams considering effect of sizes and shapes of galleries, *KSCE Journal of Civil Engineering, Vol. 20*(1), pp. 261–272. DOI: 10.1007/s12205-015-0538-2.

[5]   S.J. Dyke, J.M. Caicedo, G. Turan, L. A. Bergman, and S. Hague, 2003. Phase I benchmark control problem for seismic response of cable-stayed bridges, *Journal of Structural Engineering, Vol. 129*(7), pp. 857–872. DOI:10.1061/(ASCE)0733-9445(2003)129:7(857).

[6]   W.-X. Ren, and M. Obata, 1999. Elastic-plastic seismic behavior of long span cable-stayed bridge, *Journal of Bridge Engineering, Vol. 4*(3), pp. 1404–1412. DOI: https://doi.org/10.1061/(ASCE)1084-0702(1999)4:3(194).

[7]   A. Javanmardi, Z. Ibrahim, K. Ghaedi, and H. Khatibi, 2017. Numerical Analysis of Vertical Pipe Damper. In The 39th IABSE SYMPOSIUM; Engineering the Future, International Association for Bridge and Structural Engineering,Vancouver, Canada, Vol. 109(13), pp. 2974–2980.

[8]   H.. Ali, and A.M. Abdel-Ghaffar, 1995. Modeling the nonlinear seismic behavior of cable-stayed bridges with passive control bearings, *Computer and Structures, Vol. 54*(3), pp. 461–492. DOI: https://doi.org/10.1016/0045-7949(94)00353-5.

[9]   H.M. Ali, and A.M. Abdel-ghaffar, 1994. Seismic energy dissipation for cable-stayed bridges using passive devices, *Earthquake Engineering & Structural Dynamics, Vol. 23*(8), pp. 877–893. DOI: 10.1002/eqe.4290230805.

[10] N. Makris, 1997. Rigidity–Plasticity–Viscosity: Can electrorheological dampers protect base-isolated structures from near-source ground motions?, *Earthquake Engineering & Structural Dynamics, Vol. 26*(5), pp. 571–591. DOI: 10.1002/(SICI)1096-9845(199705)26:5<571::AID-EQE658>3.0.CO;2-6.

[11] H. Iemura, and M.H. Pradono, 2002. Passive and semi-active seismic response control of a cable-stayed bridge, *Structural Control and Health Monitoring, Vol. 9*(3), pp. 189–204. DOI:10.1002/stc.12.

[12] B.B. Soneji, and R.S. Jangid, 2010. Response of an isolated cable-stayed bridge under bi-directional seismic actions, *Structure and Infrastructure Engineering, Vol. 6*(3), pp. 347–363. DOI:10.1080/15732470701596833.

[13] A. Javanmardi, Z. Ibrahim, K. Ghaedi, M. Jameel, H. Khatibi, and M. Suhatril, 2017. Seismic response characteristics of a base isolated cable-stayed bridge under moderate and strong ground motions, *Archives of Civil and Mechanical Engineering, Vol. 17*(2), pp. 419–432. DOI: https://doi.org/10.1016/j.acme.2016.12.002.

[14] A. Javanmardi, K. Ghaedi, Z. Ibrahim, and H. Khatibi, 2016. Nonlinear seismic behavior of a based isolated cable-stayed bridge. In The 4th International Congresson Civil Engineering, Architecture & Urban Development, Shahid Beheshti University, Iran, Vol. ICSAU04_0204. Retrieved from https://www.civilica.com/Paper-ICSAU04-ICSAU04_0204.html.

[15] M. Ismail, J.R. Casas, and J. Rodellar, 2013. Near-fault isolation of cable-stayed bridges using RNC isolator, *Engineering Structures, Vol. 56*, pp. 327–342. DOI:10.1016/j.engstruct.2013.04.007.

[16] C. Bedon, and A. Morassi, 2014. Dynamic testing and parameter identification of a base-isolated bridge, *Engineering Structures, Vol.60*(2), pp. 5–99. DOI:10.1016/j.engstruct.2013.12.017.

[17] C. Christopoulos, and A. Filiatrault, eds., *Principles of Passive Supplemental Damping and Seismic Isolation*, IUSS Press, Pavia (Italy), 2006.

[18] D. Janjic, M. Pircher, and H. Pircher, 2003. Optimization of cable tensioning in cable-stayed bridges, *Journal of Bridge Engineering, Vol. 8*(3), pp.131–137. DOI:10.1061/(ASCE)1084-0702(2003)8:3(131).

[19] AASHTO, 2010. Guide Specifications for Seismic Isolation Design, Third, American Association of State Highway and Transportation Officials, Washington DC.

[20] AASHTO, 2012. LRFD Bridge Design Specifications, American Association of State Highway and Transportation Officials, Washington DC.

[21] Somerville, Paul G.; Smith, Nancy F.; Punyamurthula, Sujan; Sun, Joseph I., 1997. Development of ground motion time histories for phase 2 of the FEMA/SAC Steel Project. SAC Joint Venture, Sacramento, California.

[22] A. Filiatrault, R. Tinawai, and B. Massicotte, 1993. Damage to cable-stayed bridge during 1988 saguenay earthquake. II: Dynamic analysis, *Journal of Structural Engineering, Vol. 119*(5), pp. 1450–1463. DOI: 10.1061/(ASCE)0733-9445(1993)119:5(1450).

Bending Strength of Steel Fibre Reinforced Concrete Ribbed Slab Panel

Amir Syafiq Samsudin, Mohd Hisbany Mohd Hashim[1], Siti Hawa Hamzah and Afidah Abu Bakar

Faculty of Civil Engineering Universiti Teknologi MARA
Shah Alam, 40450 Selangor Darul Ehsan
[1]E-mail: hisbany@salam.uitm.edu.my

ABSTRACT

Nowadays, demands in the application of fibre in concrete increase gradually as an engineering material. Rapid cost increment of material causes the increase in demand of new technology that provides safe, efficient and economical design for the present and future application. The introduction of ribbed slab reduces concrete materials and thus the cost, but the strength of the structure also reduces due to the reducing of material. Steel fibre reinforced concrete (SFRC) has the ability to maintain a part of its tensile strength prior to crack in order to resist more loading compared to conventional concrete. Meanwhile, the ribbed slab can help in material reduction. This research investigated on the bending strength of 2-ribbed and 3-ribbed concrete slab with steel fibre reinforcement under static loading with a span of 1500 mm and 1000 mm x 75 mm in cross section. An amount of 40 kg/m steel fibre of all total concrete volume was used as reinforcement instead of conventional bars with concrete grade 30 N/mm². The slab was tested under three-point bending. Load versus deflection curve was plotted to illustrate the result and to compare the deflection between control and ribbed slab. This research shows that SFRC Ribbed Slab capable to withstand the same amount of load as normal slab structure, although the concrete volume reduces up to 20%.

Keywords: *steel fibre, ribbed slab, multiple ribbed slab*

INTRODUCTION

Reinforced concrete can be explained as a concrete that mixed with strong material such as steel which increase its strength under tension and make it less likely to fail. It is also a long-lasting building material that can be produced in various sizes and shapes. Its effectiveness and flexibility can be achieved by combining the best features of concrete and steel [1]. Due to the global changes in the economy, especially in the construction industry these days, it is observed that there are rapid increments in material price which at the same time causes the rapid hikes of the structure value especially those in urbanised areas. Therefore, it is important to find alternatives to reduce the quantity of material whilst constructing something that can carry the same function to the before-product.

However, in return of constructing a structure using less quantity of materials, there comes another concern related to its strength and capability to withstand load. Upon reducing the quantity of material for a structure, the strength of that particular structure will also reduce along with it. Due to the stated problem, fibre made of steel, glass and others are used to assist the structure. Different fibres have different characteristics, thus have different effects on concrete. Fibre reinforced concrete can effectively reduce the brittleness of concrete and improves its characteristics. Steel fibre is the commonly used fibre [2-3]. Steel fibre can increase the toughness of concrete as well as its resistance to impact.

Moreover, the cost of construction can be reduced when steel fibre is mixed in plain concrete [4]. With the addition of steel fibre, the ultimate load may increase up to 13% with a 3% reduction of displacement compared to normal concrete slabs [5]. During full-scale testing on the central loaded ground slab, it showed that the addition of steel fibre increased the load carrying capacity of the structure [6]. Steel fibre reinforced concrete is a concrete with added amounts of steel fibre [2][7].

Numerous researches have been conducted on the use of steel fibre on slab structures [5][8]. From previous research, hooked end steel fibre was found to be a suitable additional material to improve the performance of concrete such as mechanical resistance of concrete and ductility [9]. Steel

fiber also improved the bond and anchorage of the steel fibres in concrete mixtures [10].

Strength and stiffness of structure depend on the strength and toughness of joint between layers. Therefore, ribs and other various shapes are included in order to help reduce the cost of the structure. The variety of design of the slab structure can reduce the concrete use up to 30% and give good strength [11]. Ribbed slab introduces void at the soffit to reduce its dead weight and increase the efficiency of the concrete section. With the variety of design such as ribbed slab and waffle slab, it is as an advantage in architectural design and also economic in term of material use [12]. Part of the benefit of ribbed slab is its lightweight nature. If the structure is lightweight, the support for the slab will also reduce, thus reducing the usage of material such as concrete for other structures such as beam and column. The ribbed slab can also provide extra strength in one direction of the slab.

In research done using finite element analysis, the behaviour of ribbed slab is similar to normal concrete structure. This is due to the addition of steel fibre in concrete mix [13].

The ribbed slab can also help in improving the aesthetical value of a structure. For example, instead of using the normal, rectangular slab, ribbed slab can be used as a substitute without losing the strength needed to give a fresh look to the old rectangular slab. Ribbed slab is seen as simpler in terms of design and also easier to cast on-site.

EXPERIMENTAL

Two-ribbed slab samples and one normal slab were cast in this work having the same concrete grade of 30 N/mm². Furthermore, the dimension of all the specimens were identical in term of size. Figure 1 shows the cross-sectional dimensions of the both SFRC, 2 and 3-ribbed slabs, and Figure 2 shows the plan view of SFRC ribbed slab with depth 75 mm by width 1000 mm and length is 1500 mm. In addition, because those slabs were ribbed slabs, there were voids created below the slabs. For two-ribbed slabs, there are

2-ribbed which each rib was made with a size of 37.5 mm by 335 mm and the size of the void is 37.5 mm by 200 mm in depth and width respectively. Meanwhile, for 3-ribbed slabs, there are 3 ribbed which each rib was made with a size of 37.5 mm by 200 mm and the size of the void is similar to the size of rib. All the ribs have same length as the slab which is 1500 mm.
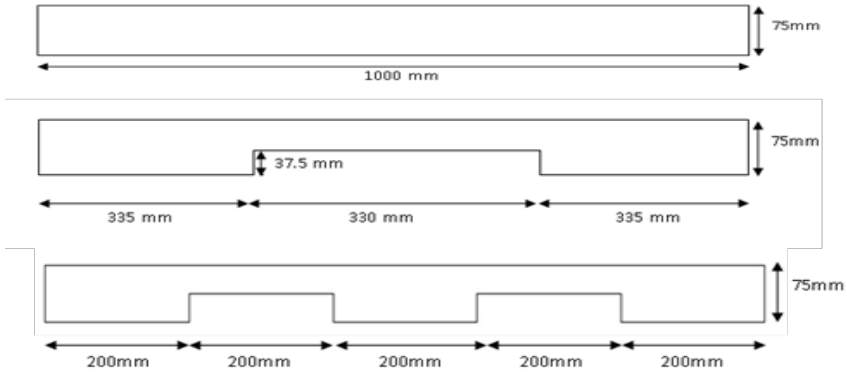
Figure 1: Control and Ribbed Slab Dimension (source by author)
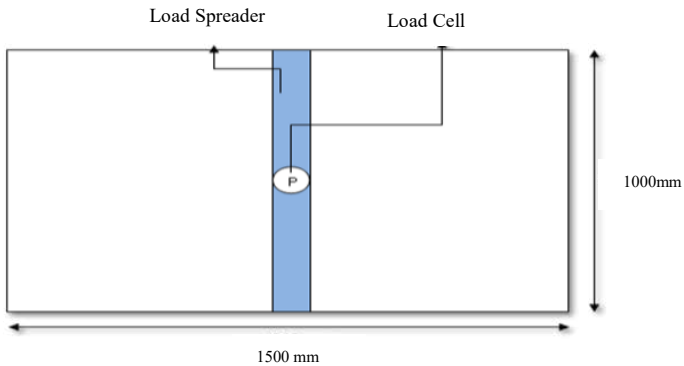
Figure 2: The Plan View of SFRC Ribbed Slab (source by author)

Mixing of concrete was done thoroughly to ensure that concrete of uniform quantity is obtained. For this study, the machine mixing was done in casting of concrete up to 0.1 m³. Initially, the surface of formwork waslevelled and moist by oil. After that, the coarse aggregates were spread over the sand, and then the cement was spread over course aggregate. The

mixer was operated up to two minutes for mixing until the colour of the mixture is uniform. Then, the water was added slowly while the mixer was operating until the mixture obtains proper consistency. The steel fibres were added last into the mixture gradually until it is well distributed.

Three Points Bending Test

Bending test was conducted to determine the strength of a material when bent over a given radius. Three point bending test is selected due to its simplicity and it is suitable to evaluate fibre reinforced concrete properties [13]. Using the universal testing machine, the slab was placed in the set-up to test its ultimate strength. One of the main advantages of three points bending testing is the ease of testing. Four LVDTs were placed at the centre, upper part and lower part of the slab.

Both Figure 3 and Figure 4 shows the placement of load in two types of view which used the three point load test using the machine. The load applied was gradually increased until the slab fails and the data logger recorded its ultimate strength. In addition, there were also four LVDTs used in this study for each specimen to obtain the displacement or deflection of concrete. The LVDT placed on both top and bottom surfaces of the slab, where each surface placed two of the transducers. Figure 5 shows the detailed locations of each transducer. Figure 6 shows the actual settings done at the Heavy Laboratory.
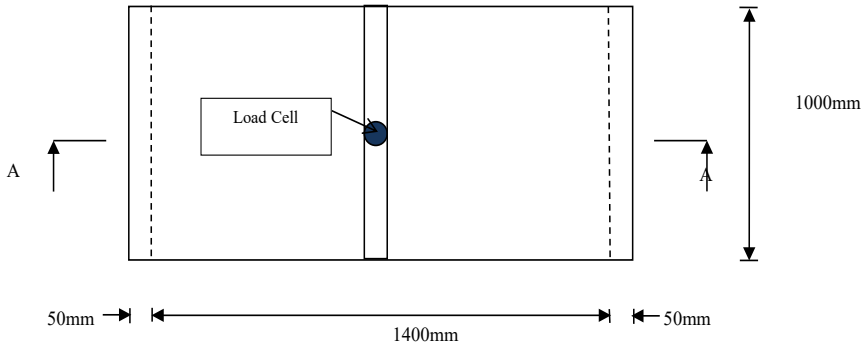
Figure 3: Plan View of Experimental Setup (source by author)
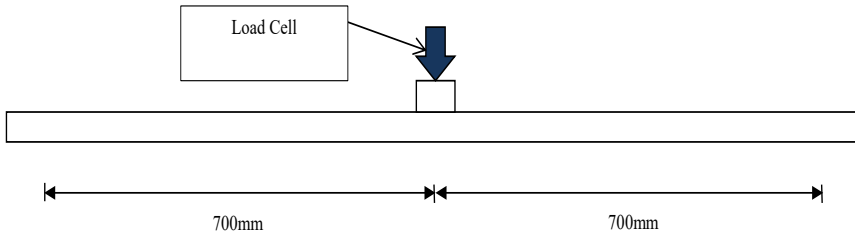
Figure 4: Side Elevation View of Experimental Setup (source by author)
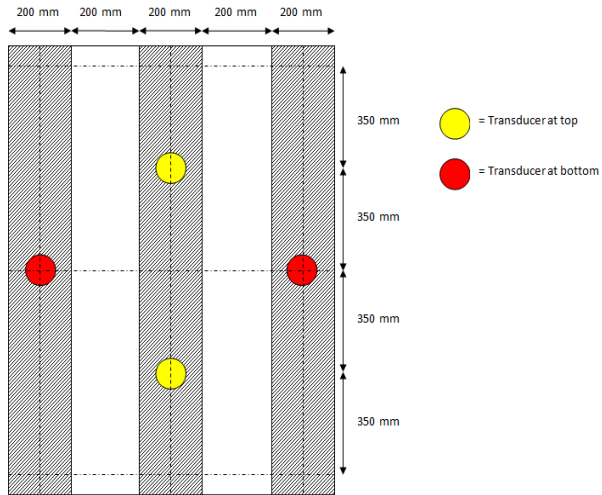
Figure 5: Position of LVDT (source by author)

Figure 6: Laboratories Experimental Setup (source by author)

Before testing, the dimension of the setup was carefully checked, and a detailed visual inspection made with all information was carefully recorded. After setting and reading all gauges, the load was increased incrementally up to calculated working load, with loads and deflections recorded at each stage. Loads were increased normally again in similar increments up to failure as well as deflection be recorded too.

RESULT AND DISCUSSION

Load versus Displacement

The results illustrated in Figure 7 show that the load has been increased up to its failure level, then, load and deflections for all the load steps wererecorded. Each slab shows different behaviour when the load was applied to them. Initially, there is a not much difference from both slabs when the load started to apply. But, the 2-ribbed slab shows it can cater much load at the beginning of the test compared to the 3-ribbed slabs. It is observed that the 2-ribbed slab behaved linearly elastic up to the value of around 5.97 kN higher 23.11% compared to the 3-ribbed slab recodring 4.59 kN where at this point, the minor cracks started appear at the tension face of the bottom slab. As the load further increases, the deflection started increasing with the load increment up to maximum load. The ultimate

carrying capacity of the 2-ribbed slab is 6.2 kN when the deflection has reached to the value of 0.82 mm, while 5.97 kN and 4.81 mm of ultimate load and deflection for 3-ribbed slab respectively. After reaching the ultimate load, the value of load decreases as the slab losses its stiffness or the slab facing the softening stage.
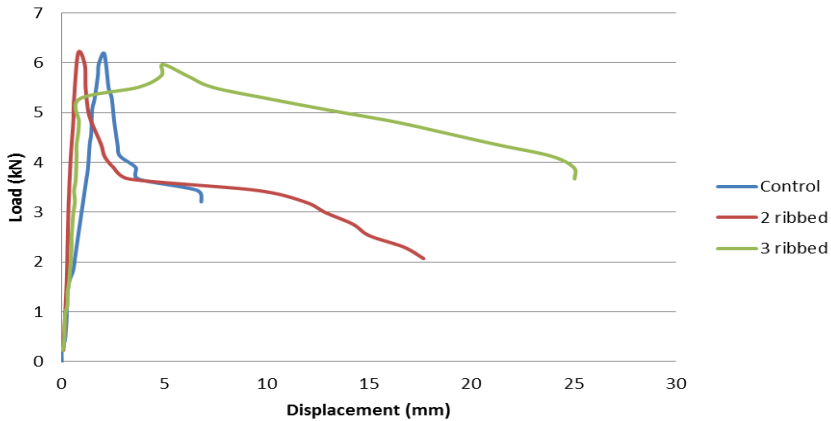
Figure 7: Load versus Deflection (source by author)

Table 1 tabulates the maximum load and deflection for control, 2-ribbed slab and also 3-ribbed slabs. The maximum deflection recorded from the test shows that control slab achieved the value of 2.04 mm of displacement at the highest load of 6.2 kN which behave similarly with 2-ribbed slab in term of maximum loading which is 6.2 kN with the displacement recorded is 0.82 mm. In the meantime, 3-ribbed slab recorded the maximum load of 5.97 kN and the deflection at maximum loading around 4.81mm.

Table 1: Maximum Load and Deflection

Sample	Maximum Load (kN)	Deflection at Maximum Load (mm)
Control	6.2	2.04
2-Ribbed	6.2	0.82
3-Ribbed	5.97	4.81

From the results shown in Figure 7 and Table 1, it is observed that the 2-ribbed slab behaved linearly elastic up to the value of around 5.97 kN higher 23.11% compared to the 3-ribbed slab marked 4.59 kN where at this point the minor cracks started to appear at the tension face of the bottom slab. As the load further increases, the deflection started to increase with the load increment up to maximum load. The ultimate carrying capacity of the 2-ribbed slab is 6.2 kN when the deflection has reached to the value of 0.82 mm, while 5.97 kN and 4.82 mm of ultimate load and deflection for the 3-ribbed slab respectively. After it reaches the ultimate load, the value of load decreases as the slab losses its stiffness or the slab facing the softening stage.

There are several factors that lead to the results. Firstly, the bonding between concrete and steel fibres affects the behaviour of slabs. Based on this study, the steel fibres functions well to extend or postpone the disintegration of matrix concrete because the tensile stress was absorbed by steel fibre. Furthermore, using of hooked-end fibre shows the effectiveness of elastic state of SFRC ribbed slabs. The hooked-end steel fibres tie the concrete effectively. During the elastic stage, the steel fibre plays an important role to maintain the concrete elastic behaviour longer than normal concrete [5]. In order for the SFRC to continue to carry the load and deform plastically after cracking has occurred, it is essential for the fibers to be sufficiently anchored in the concrete matrix to enable the full tensile strength of the fibres to be harnessed. Physical testing of steel fibres for pullout values has shown that 'hooked-end' fibres pull through as the ultimate fibre capacity is reached and this means the full capacity of the fibre is achieved over high deformations giving high-energy absorption and the characteristic ductility required to prevent brittle failure [5][9].

From the deflection magnitude, 2-ribbed slab is lower compared to 3-ribbed slab. Actually, this condition is unexpected condition where logically, the deflection will increase as the load increases. The reason of this is maybe due to the rib plays the role to control the deflection of the slab. So, the increasing number of ribs can reduce the slab deflection. In addition, because this slab is designed as ribbed slab, the depth of rib also can influence the deflection of the slab. The ribbed slab can act like a beam. The ribbed depth influences the slab deflection. In this study, the rib depth of both slabs is only 75 mm where the width of ribs is 200 mm and

330 mm respectively. Normally, the ratio depth over width is taken into account to design rib of the slab. Actually, the best range ratio d/b (depth/breadth) is between two to three. The ratio became higher if the depth of rib increases. Unfortunately, for this test the slab cannot be designed with higher depth because the limitation of formwork for cast thicker slab. And also, if the ribbed depth increases, the rib can lead to shear failure. Shear crack can only be prevented by putting a shear bar inside the ribs. However, has not been experemente to avoid using any conventional bar for tensile and shear resistance. Perhaps, this slab can maintain the depth of ribbed, but the breadth of rib need to be reduced as close as to the best of d/b ratio. When the width of ribbed is smaller, the amount of concrete used also can be reduced. Indirectly, the self-weight of the slab can be kept low.

Visual Inspection

During the static load test, all the cracks formed were recorded. Loading was applied at mid span of the slab specimen. As the load increased, crack slowly appeared and its pattern visible to naked eyes. Crack patterns are one of the information that was observed.

From Figures 8, 9, and 10, it can be observed that each slab specimen displayed different crack pattern. For control and 2-ribbed slab, the crack pattern of the slab almost straight line as compared to the 3-ribbed slab which scattered along the neutral axis.

However, the crack for control appeared to be far from the neutral axis compared to the 2-ribbed slab when the crack drifted slightly away from neutral axis. This situation happened because of the uneven slab surfaces. When the load was applied, the crack started to disperse and propagated away from the neutral axis.

Figure 8: Crack Pattern of Failed Control Slab (source by author)

Figure 9: Crack Pattern of Failed Two-Ribbed Slab (source by author)

Figure 10: Crack Pattern of Failed Three-Ribbed Slab (source by author)

As compared to control and 2-ribbed slab, the crack width of 3-ribbed slab more deeper and wider. Due to the effect of steel fibres, the slab specimens did not break up completely. These fibres are usually used to control the effect of cracking and shrinkage, thereby it also improved its toughness. Fibre acts as crack arresters through the initial loading stage, and increase energy required for crack propagations, that provide the increase in strength [15].

CONCLUSION

Steel Fiber Reinforced Concrete (SFRC) can be one of the structural materials which has potential in the construction industry. The behaviour of SFRC ribbed slabs in this study showed that there is slightly different between normal concrete and ribbed slab in term of ultimate load carrying capacity and the magnitude of deflection.

The result shows that the steel fibre inside concrete plays important role to absorb more loads even though there is no reinforcement added. From the experiment, the load capacity from both slabs was found to be below 10 kN. But, if compared with normal reinforced concrete slab, this study proves the steel fibres can act as reinforcement for concrete structure. The following conclusions are drawn based on the experimental reselut tested on SFRC ribbed slabs:

a) The ultimate strength for 2-ribbed slabs is similar to control slab where the reduction of materials has resulted in both slabs behaves almost the same with the control slab. This shows that upon reducing the amounted materials, it only affects the strength of the material at a very small scale.
b) The SFRC 2-ribbed slab has greater 37.4% ultimate load capacity and lower 82.9% deflection compared to 3-ribbed slab.
c) Compared to the previous research using numerical analysis, the maximum load capacity of the same sample, it was found that the numerical value and experimental value is similar.
d) It is found that, steel fibre does effectively function as crack arrestor. This can be seen in the crack pattern on the failed ribbed slab.

ACKNOWLEDGEMENT

REFERENCES

[1]   B., Mosley, J., Bungey and R., Hulse, 2012. *Reinforced Concrete Design to Eurocode 2*. 7th Edition. London: Palgrave Macmillan.

[2]   N., Abdul Rahman, S. H., Hamzah, and E. T. Wong, 2008. Effective performance of steel fibre reinforced concrete wall panel for IBS component. In *International Conference of Construction and Building Technology* (ICCBT), pp 203-212.

[3]   A.R., Jamilah, H. Siti Hawa, and M. S., Hamidah, 2015. Expanded polystyrene fibred lightweight concrete (EPSF-LWC) as load bearing wall, *Jurnal Teknologi, Vol. 76*(9), pp. 81-85. DOI: https://doi.org/10.11113/jt.v76.5656.

[4]   M. N. S., Hadi, 2008. An Investigation of the Behaviour of Steel and Polypropylene Fiber Reinforced Concrete Slabs. University of Wollongong. Retrieved from http://ro.uow.edu.au/engpapers/477.

[5]   A.R., Nurhaniza H., Siti Hawa, and A., Abdulrazzaq, 2012. Effectiveness of SteFib in composite structural member, *Journal of Engineering Science and Technology, Vol. 7*(5), pp. 552-562.

[6]   Timuran Engineering Sdn. Bhd., 2007. How to Choose Your Required Steel Fibres, *IEM JURUTERA Buletin*. 4, 32.

[7]   V. C., Ngu, 2004. Seminar Material. Lecture, Ho Chi Minh: Faculty of Civil Engineering, Ho Chi Minh City University of Techology.

[8]   J.B., De Hanai, and K.M.A., Holanda, 2008. Similarities between punching and shear strength of steel fiber reinforced concrete (SFRC) slabs and beams, *Revista IBRACON Structures and Materials Journal, Vol. 1*(1), pp. 1-16. DOI: http://dx.doi.org/10.1590/S1983-41952008000100001.

[9]   J.F., Lataste, M., Behloul, and D., Breysse, 2008. Characterisation of fibres distribution in a steel fibre reinforced concrete with electrical resistivity measurements, *NDT & E International, Vol. 41*(8), pp. 638-647. DOI: https://doi.org/10.1016/j.ndteint.2008.03.008.

[10]   S.A., Altoubat, J.R., Roesler, D.A., Lange, and K., Rieder, 2008. Simplified Method for Concrete Pavement Design with Discrete Structural Fibres, *Journal of Construction and Building Materials, Vol. 22*(3), 384-393. DOI: https://doi.org/10.1016/j.conbuildmat.2006.08.008.

[11]   P., Mindaugas & V., Juozas, 2010. Analysis of Bending Capacity of Composite Steel-Concrete Slabs with Steel Fiber Reinforced Concrete. In *The 10th International Conference,* Vilnius, Lithuania 19-21 May 2010.

[12]   H.M.S., Abdul-Wahab, and M.H., Khalil, 2000. Rigidity and Strength of Orthotropic Reinforced Concrete Waffle Slab, *Journal of Structural Engineering, Vol. 126*(2), pp 219-227 DOI: 10.1061/(ASCE)0733-9445(2000)126:2(219).

[13]   A. S., Samsudin, M. H. M., Hashim, S. H., Hamzah, A. A. Bakar, M. F. Mohamed, 2015. Modelling of steel fibre reinforced concrete ribbed slab under multiple ribbed conditions, *Advanced Materials Research, Vol. 1134*, pp. 127-130. DOI: https://doi.org/10.4028/www.scientific.net/AMR.1134.127.

[14] E., Sideridis, and G. A., Papadopoulos, 2004. Short-beam and three-point-bending tests for the study of shear and flexural properties in unidirectional-fiber reinforced epoxy composites, *Journal of Applied Polymer Science, Vol. 93*(1), pp. 63–74. DOI: 10.1002/app.20382.

[15] G., Martinez-Barrera, F., Urena-Nunez, O., Gencel, and W., Brostow, 2010. Mechanical properties of polypropylene-fiber reinforced concrete after gamma irradiation, *Composites Part A Applied Science and Manufacturing, Vol. 42*(5), pp. 567-572. DOI: 10.1016/j. compositesa.2011.01.016.

Preliminary Investigation on the Flexural Behaviour of Steel Fibre Reinforced Self-Compacting Concrete Ribbed Slab

Nur Aiman Suparlan, Muhammad Azrul Ku Ayob, Hazrina Ahmad[1], Siti Hawa Hamzah, Mohd Hisbany Mohd Hashim

Faculty of Civil Engineering, Universiti Teknologi MARA
40450 Shah Alam, Selangor, Malaysia
[1]E-mail: hazrinaahmad@gmail.com

ABSTRACT

A ribbed slab structure has the advantage in the reduction of concrete volume in between the ribs resulting in a lower structural self-weight. In order to overcome the drawbacks in the construction process, the application of steel fibre self-compacting concrete (SCFRC) is seen as an alternative material to be used in the slab. This preliminary investigation was carried out to investigate the flexural behaviour of steel fibre self-compacting concrete (SCFRC) as the main material in ribbed slab omitting the conventional reinforcements. Two samples of ribbed slab were prepared for this preliminary study; 2-ribbed and 3-ribbed in 1 m width to identify the effect of the geometry to the slab's flexural behaviour. The dimension of both samples is 2.5 m x 1 m with 150 mm thickness. The compressive strength of the mix is 48.6 MPa based on the cubes tested at 28 days. Load was applied to failure by using the four point bending test set-up with simple support condition. The result of the experiment recorded ultimate load carrying capacity at 30.68 kN for the 2-ribbed slab and 25.52 kN for 3-ribbed slab. From the results, the ultimate load of the 2-ribbed sample exceeds 3-ribbed by approximately 20%. This proved that even with lower concrete volume, the sample can still withstand an almost similar ultimate load. Cracks was also observed and recorded with the maximum crack width of 2 mm. It can be concluded that the steel fibres do have the potential to withstand flexural loadings. Steel fibre reduces macro-crack forming into

micro-cracks and improves concrete ductility, as well as improvement in deflection. This shows that steel fibre reinforced self-compacting concrete is practical as it offers good concrete properties as well as it can be mixed, placed easier without compaction.

Keywords: *ribbed slab, steel fibre reinforced self-compacting concrete, hooked end, flexural, crack*

INTRODUCTION

Ribbed slab is a structure that consists of ribs spanning in one way and connected by structural concrete topping. The ribs are arranged in longitudinal direction and behave similarly to beams. The main advantage of the ribbed slab application is the reduction of the total structures weight by the removal of the concrete part below the neutral axis. This type of slab is suitable for the application in structures with light or moderate imposed loads, such as the hospital wards, school buildings and apartments [1].

Despite of the numerous advantages of a ribbed slab structure, there are drawbacks on the effectiveness of the ribbed slab especially in terms of its construction method. A ribbed slab that consists of small multiple ribs leads to the requirement of special formwork, complication in the placement of the reinforcements as well as improper concrete compaction [2]. The application of self-compacting concrete (SCC) in the construction of precast ribbed slab panel is seen as an alternative solution to the complication in placing the reinforcement with effective compaction of concrete in the ribs. Therefore, the development of the SCC that is high in flow and workability has been identified as an effective replacement to the conventional concrete used in construction industry that is dependent on the quality of the construction work [3].

The main advantages of SCC is its ability to be properly poured in place, filling the formwork corners and small voids between reinforcement bars by means of its own weight [3]. Its rheological property allows SCC

to be effectively applied in complex shaped elements and congested reinforcements [4]. The engineering and mechanical properties of the hardened SCC is reported by a number of researchers to be almost similar to the ordinary well compacted concrete [5-7].

Plain concrete is a quasi-brittle material. Therefore, steel fibres are incorporated in the concrete mix in order to improve this behaviour and produce a more ductile material. However, the addition of steel fibres affects the workability of the fresh concrete significantly cause the mix to be much stiffer with lower slump measurement causing the mixture to be less workable [8]. Stiffer mixes further causes uneven distribution of steel fibres in the mix, whereas uniform fibre dispersion is very important especially for the structural application. The compaction process that is performed in the concrete casting process might also disturb the homogeneity of the steel fibre dispersion [9]. Therefore, by taking advantage of the rheological performance of self-compacting concrete (SCC) at fresh state, steel fibres are added to the mix to produce self-compacting steel fibre reinforced concrete (SCFRC) with a more uniform fibre dispersion in a highly workable mixture [4].

Steel fibres have been successfully used in concrete to improve its mechanical properties, such as post-cracking, load bearing capacity and energy absorption performance. Higher fibre volume in the mix results in an increment in the residual flexural strength, flexural toughness, energy absorption as well as the load bearing capacity by the fibre knitting between cracks that allows stress transfer at the crack openings [10-11]. Fibres are also used to limit the crack width, with beneficial consequences in terms of concrete durability. Apart from that, steel fibre can extend the technical benefits of SCC by providing crack bridging ability, higher toughness and long term durability.

EXPERIMENTAL WORK

The experimental work was carried out at the Heavy Structural Laboratory in Universiti Teknologi MARA, Malaysia. Two slab samples were prepared to assess the flexural behaviour of SCFRC in ribbed slabs, varying in the

number of ribs; 2-ribbed and 3-ribbed as shown in Figure 1(a) and (b). Both samples were prepared with similar dimensions of 2.7 m x 1 m with the effective length of 2.5 m. The volume of ribbed slab constructed in this research is lesser than solid slabs due to the presence of void. The savings of the concrete volume is up to 14% and it is presented in Table 1.

Table 1: Percentage of Concrete Volume Reduction

Type of slab	Concrete volume (m³)	% of concrete volume reduction
Solid	0.375	0 %
2-ribbed	0.323	14 %
3-ribbed	0.334	11 %

For this research, mix was prepared in accordance with the mix design in Table 2. The type of steel fibres used is hooked end with the tensile strength of 1100 MPa; measuring 0.75 mm in diameter and 60 mm in length as shown in Figure 2. The fibres were included in the mix by volume fraction of 0.5% amounting to 40 kg/m³.
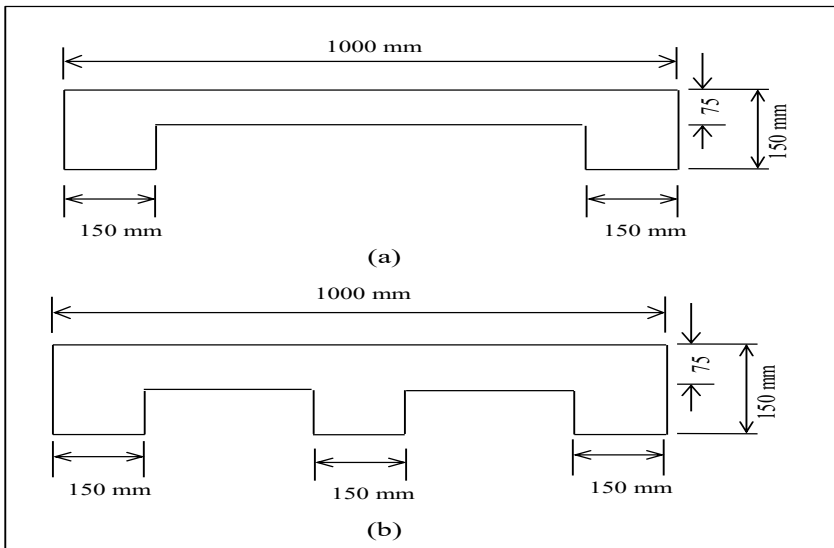
Figure 1: Slab Sample Dimensions; (a) 2-ribbed (b) 3-ribbed (source by author)

Figure 2: Hooked End Steel Fibre (source by author)

Table 2: Mix Design of SCFRC

Content	kg/m3	Remarks
Cement	465	CEM I 52.5 R
Fly ash	85	15%
Coarse aggregates	590	Maximum size 16 mm
Fine aggregates	910	Maximum size 5 mm
Water	227.7	w/p = 0.41
Steel fibres	40	0.5%
Superplasticizer	Glenium ACE 8589	0.75l / 100 kg binder

With regards to the self-compacting concrete rheological properties, the slump flow test was performed before the mix was poured into the formwork. This procedure was carried out to verify the ability of the mix to spread and self-compact without any vibration. Cubes were cast to measure the compressive strength of the mix used in this study.

The ribbed slab samples were tested under four- point bending test in accordance with the BS EN 12390:5 [12]. Conventional steel reinforcement bars or wire mesh were not provided in the samples in the attempt to fully assess the effectiveness of the steel fibres under flexure. Figure 3 shows the experimental setup of the experiment. Circular steel rollers were used to apply the loads on the ribbed slab. Figure 4 shows the arrangement of the loads applied to the slab samples. The loads were placed at two positions demonstrating the four-point bending load condition.

For the purpose of deflection measurement, linear variable displacement transducers (LVDT) were engaged to the ribbed slab sample at critical locations. The location of the LVDTs for the 2-ribbed and 3-ribbed slabs are shown in Figure 5(a) and (b), respectively.
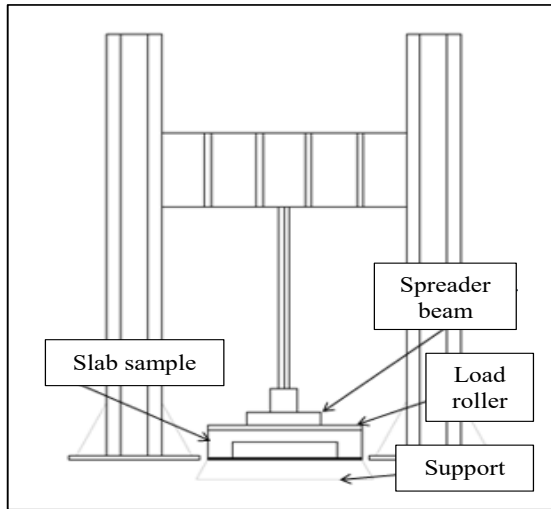
Figure 3: Experimental Setup (source by author)
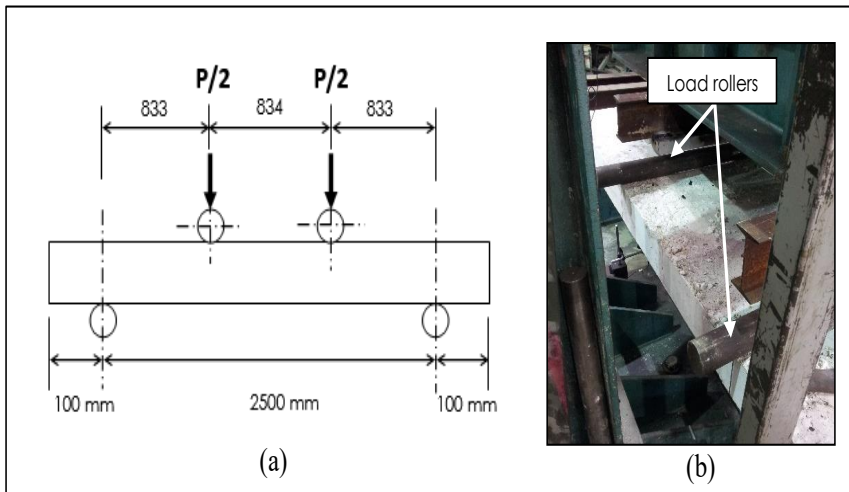
Figure 4: Loading Arrangement; (a) Schematic Diagram and (b) Laboratory Photograph (source by author)
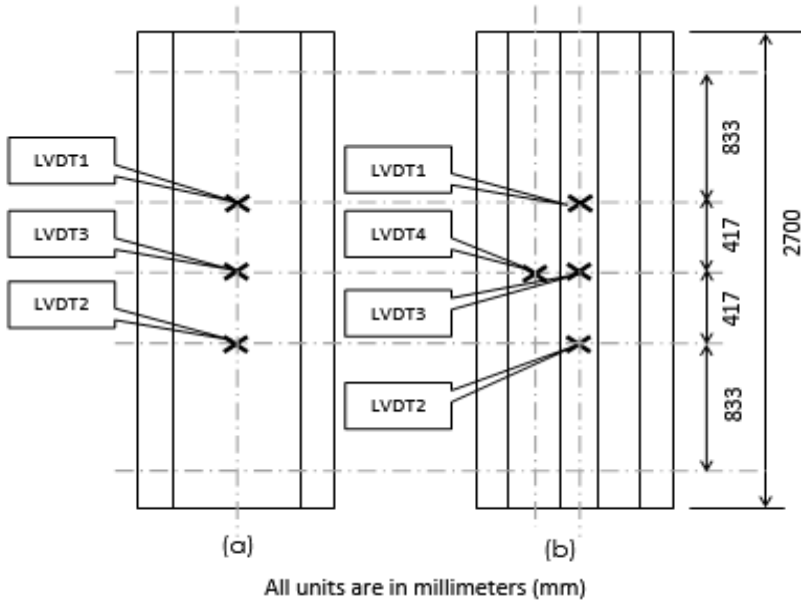
Figure 5: LVDT Locations; (a) 2-ribbed (b) 3-ribbed (source by author)

RESULTS AND DISCUSSION

Slump flow

Slump flow test was performed to assess the flow ability and flow rate of the SCC mix without any obstacle [13]. Table 3 shows the slump flow result from the experiment. From the results of the slump flow test, it can be observed that the slump flow and t500 of the plain SCC mix fulfilled the European Federation of National Associations Representing for Concrete (EFNARC) requirement [14]. However, as 0.5% steel fibres were added to the mix, the slump flow and t500 was significantly affected. Based on visual observation, the mix appear to be less viscous with the addition of the fibres. The steel fibres restrained the movement of the aggregates in the mix [15]. This behaviour is also attributed to the hooked end type of fibres as well as the dimension that is relatively large that causes blockage of the particles as it flows [16].

Table 3: Slump Flow Results

	Plain SCC	SCFRC
Slump flow (mm)	650	580
t500 (sec)	4	7

Compressive Strength

The compressive strength of the concrete mix used in the experiment is as shown in Figure 6. The characteristic strength of the SCC mix is 30 N/mm² with the target mean strength of 43 N/mm². The cubes were tested at 7 and 28 days.

Figure 6 shows the compressive strength of the cubes. At 28 days, the compressive strength exceeded the target mean strength by approximately 15%. This might be due to the type of cement used in the mix, which is CEM I 52.5R (Portland cement with high initial strength) as well as the high amount of cement.

In comparison of steel fibres provision, the results reveal that the compressive strength of cubes with steel fibres were lower than plain SCC without fibres. The reduction in strength with the addition of the steel fibres might be due to the decrease in the workability of the concrete[15][17]. A more viscous mix could be clearly observed in the slump flow results as reported in the previous section. This reduction might also be attributed to the disturbance cause by the steel fibres to the SCC matrix producing additional voids in the samples resulting lower compressive strength [15].
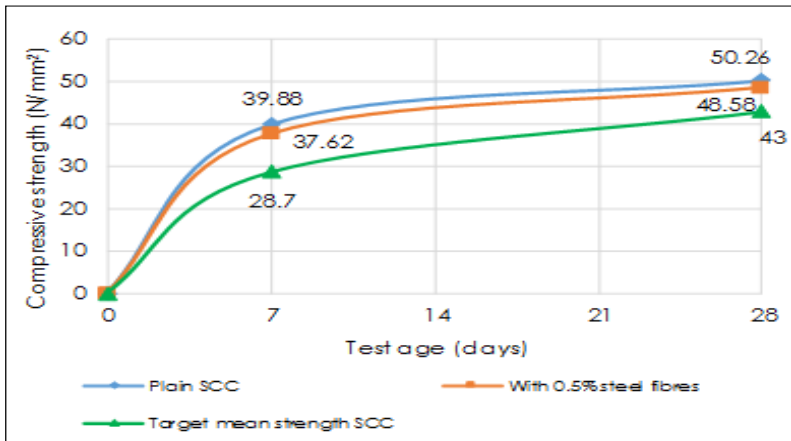
**Figure 6: Compressive Strength of Concrete Cubes at 7 and 28 Days
(source by author)**

Ultimate Load Carrying Capacity and Deflection

Figures 7and 8 show the graphs of load-deflection for the 2-ribbed and 3-ribbed slab tested by the four-point bending test. The results showed that the ultimate load of the 2-ribbed and 3-ribbed slab samples were 30.68 kN and 25.52 kN, respectively. The ultimate load of the 2-ribbed slab exceeded that of 3-ribbed at approximately 20%.

It exhibits that the 2-ribbed slab sample has the ability to withstand an almost similar load that can withstand by the 3-ribbed despite of its lesser volume of concrete as presented in Table 1. This might have been the result of a small difference between the concrete volumes that shows only 3% difference resulting almost equivalent load bearing capacity between these two samples. Therefore, since the steel fibres functions as the only reinforcement in the slab, the volume plays an important role in affecting the load bearing capacity of each sample.

Referring to Figure 7, the 2-ribbed slab sample showed almost similar curves for readings from LVDT 1 and 2 which is located under the load, the location as shown in Figure 5(a) recorded maximum deflection of 9.61 mm. All three transducers were placed at the bottom of the slab topping. Meanwhile, readings from LVDT 3 show a drastic drop with stagnant deflection at approximately 31 kN load. This might be attributed to the failure of the slab that caused the LVDT to abruptly lose its readings.

The results of the 3-ribbed slab sample are presented in Figure 8. Readings from LVDT 1, 2 and 4 show similar curves reaching maximum deflection of 25.12 mm. The maximum deflection value was recorded at the location of LVDT4 which is placed at the bottom of the slab topping which is similar to the 2-ribbed slab sample. At peak load, the slab deflects to a magnitude of 5.09 mm for the 2-ribbed slab while for the 3-ribbed, the deflection is smaller, achieving 3.82 mm. This result again shows that the 2-ribbed has almost similar performance as the 3-ribbed slab.

Based on the load-deflection graphs of both slab samples, it can be observed that the loads experienced a gradual decrease after achieving the ultimate load with an almost similar pattern. The gradual decrease was due to the effective bonding of the hooked ends fibres to the SCC matrix [5]. The graphs has proved that both slabs similarly experienced deflection softening [5][18] which is expected in the behaviour of steel fibre reinforced concrete material. However, the curve for the 2-ribbed slab is steeper as compared to the 3-ribbed slab.

The steep curve resulted from the failure of the 2-ribbed slab. At approximately 15 kN, the slab broke into two parts. The 3-ribbed slab showed a more gradual decrease of load and the curve extends further without causing sudden failure to the slab. This is due to the presence of the internal rib that assists in sustaining the subjected loads. This has proved that the steel fibres in the 3-ribbed slab have effectively bridge the cracks by holding the matrix together rather than allowing the structure to undergo brittle and sudden failure.
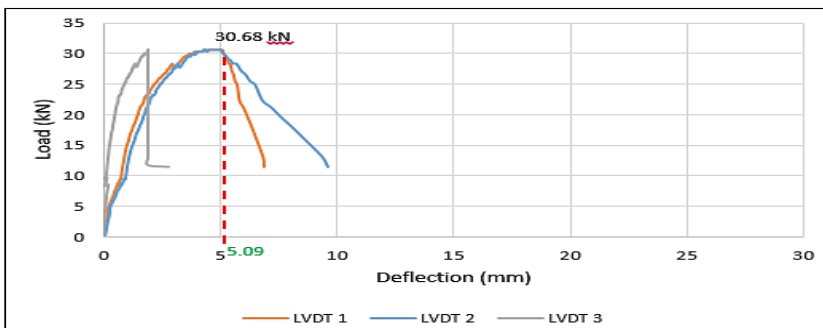
Figure 7: Load Versus Deflection Graph of the 2-Ribbed Slab (source by author)
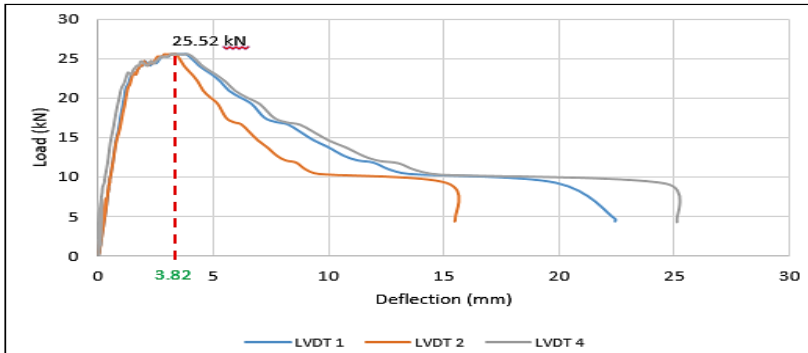
Figure 8: Load Versus Deflection Graph of the 3-Ribbed Slab (source by author)

Crack Propagation and Failure Modes

As the load imposed to the slab samples, visual observation was made to observe the crack propagation and its location. The crack was initiated at the bottom part of the ribs that is subjected to the highest tensile stress for both samples. The slab topping that is in the compression zone had manage to withstand the loads as no cracks was observed at the early stage. The cracks at the bottom of the ribs continued to propagate towards the top surface as the load progresses. Cracks were generated in the area of the mid span where the highest moment occurs. Table 5 shows the crack width of both samples.

Table 5: Crack Width of Ribbed Slab

Sample	Crack width (mm)
2-Ribbed Slab	1.55
3-Ribbed Slab	2.00

The 2-ribbed slab sample failed at the location of the load where LVDT 1 was placed. Based on visual observation, the failure might be caused by the presence of honeycombs at the top surface of the slab. The voids from the honeycombs had caused the section to easily lose its strength due to the absence of sufficient aggregates and fibres to bridge the cracks. The maximum crack width before total failure was observed to be 1.55 mm.

The failure location of the 3-ribbed sample is approximately at the mid span of the slab. The cracks started at the external rib followed by the middle rib. This is because the middle ribs is a T-section while the external are L-section. The geometry of the middle ribs provides advantage in terms of its rigidity [19]. The maximum crack length on the external rib is 175 mm while the maximum crack width is 2 mm.

From the visual observation of the crack propagation, it demonstrated that the incorporation of steel fibres in concrete has the ability to increase the energy absorption capacity of the structure, thus, improves the cracking behaviour and load bearing capacity. Cracks were formed progressively with smaller width due to the bridging effect of steel fibre that assist in clutching the concrete matrix together, increasing the ability of the structure to resist more loads.

CONCLUSION

From the results of this experiment, it can be concluded with the inclusion of 0.5% steel fibres in the SCC mix, the ribbed slab has the ability to sustain loads up to 30.68 kN and 25.52 kN, for 2-ribbed and 3-ribbed, respectively. Furthermore, the inclusion was found to effectively bridge cracks in the structure resulting a maximum of 2 mm cracks in the rib. The flexural behaviour of both ribbed slabs exhibits the deflection softening pattern with gradual decrease of load after first crack. However, the 3-ribbed slab showed a better flexural behaviour with a more gradual deflection softening curve than the 2-ribbed slab. This is observed even though the ultimate load resisted is lower. This is due to the presence of the internal rib that assists in sustaining the subjected loads.

The flexural test result shows that the steel fibres have effectively function as a restrain to the SCC matrix by still holding the slab intact even after peak load is reached avoiding sudden brittle failure of the structure. Further in depth investigation has to be carried out to determine the most optimal design of ribbed slab that can fully utilise the potential of SCFRC as reinforcements.

ACKNOWLEDGEMENT

REFERENCES

[1]   B. Mosley, J. Bungey, and R. Hulse, 2012. *Reinforced Concrete Design to Eurocode 2*, 7th Ed. London: Palgrave Macmillan.

[2]   A. Paul, 2014. Ribbed Slab System. Retrieved from http://civildigital. com/ribbed-waffle-slab-system-advantages-disadvantages/. [Accessed: 26-Feb-2015].

[3]   H. Okamura and M. Ouchi, 2003. Self-compacting concrete, *J. Adv. Concr. Technol., Vol. 1*(1), pp. 5–15. DOI: https://doi.org/10.3151/ jact.1.5.

[4]   L. Ferrara, Y.-D. Park, and S. P. Shah, 2007. A method for mix-design of fiber-reinforced self-compacting concrete, *Cem. Concr. Res., Vol. 37*(6), pp. 957–971. DOI: 10.1016/j.cemconres.2007.03.014.

[5]   M. Pająk and T. Ponikiewski, 2013. Flexural behavior of self-compacting concrete reinforced with different types of steel fibers, *Constr. Build. Mater., Vol. 47*, pp. 397–408. DOI: https://doi. org/10.1016/j.conbuildmat.2013.05.072.

[6]   M. Mithra, P. Ramanathan, P. Muthupriya, and R. Venkatasubramani, 2012.Flexural Behavior of Reinforced Self Compacting Concrete Containing GGBFS, *International Journal of Engineering and Innovative Technology (IJEIT), Vol. 1*(4), pp. 124–129.

[7] B. Persson, 2001. A comparison between mechanical properties of self-compacting concrete and the corresponding properties of normal concrete, *Cem. Concr. Res., Vol. 31*(2), pp. 193–198. DOI: 10.1016/S0008-8846(00)00497-X.

[8] S. Grünewald, 2004. Performance-based Design of Self-compacting Fibre Reinforced Concrete. Published PhD Thesis, Delft University Press.

[9] R. Gettu, D. R. Gardner, H. Salvidar, and B. E. Barragan, 2005. Study of the distribution and orientation of fibers in SFRC specimens, *Mater. Struct., Vol. 38*, pp. 31–37. DOI: 10.1617/14021.

[10] J. Michels, D. Waldmann, S. Maas, and A. Zürbes, 2012. Steel fibers as only reinforcement for flat slab construction – Experimental investigation and design, *Constr. Build. Mater., Vol. 26*(1), pp. 145–155. DOI: https://doi.org/10.1063/1.4965080.

[11] A. R. Khaloo and M. Afshari, 2005. Flexural behaviour of small steel fibre reinforced concrete slabs, *Cem. Concr. Compos., Vol. 27*(1), pp. 141–149. DOI: https://doi.org/10.1051/matecconf/201713802010.

[12] BS EN 12390-5, Testing Hardened Concrete - Part 5: Flexural Strength of Test Specimens. European Committee for Standardization (CEN) Annual Report, Brussels, March 2009.

[13] BS EN 12350-8, Testing Fresh Concrete Part 8: Self-compacting Concrete — Slump-flow Test. European Committee for Standardization (CEN) Annual Report, Brussels, 2010.

[14] EFNARC, Specification and Guidelines for Self-Compacting Concrete, Surrey, 2002.

[15] R. Madandoust, M. M. Ranjbar, R. Ghavidel, and S. F. Shahabi, 2015. Assessment of factors influencing mechanical properties of steel fiber reinforced self-compacting concrete, *Mater. Des., Vol. 83*, pp. 284–294. DOI: 10.1016/j.matdes.2015.06.024.

[16] M. Sahmaran, A. Yurtseven, and I. Ozgur Yaman, 2005. Workability of hybrid fiber reinforced self-compacting concrete, *Build. Environ., Vol. 40*(12), pp. 1672–1677. DOI: 10.1016/j.buildenv.2004.12.014.

[17] A. Khaloo, E. R. Molaei, P. Hosseini, and H. Tahsiri, 2014. Mechanical performance of self-compacting concrete reinforced with steel fibers, *Constr. Build. Mater., Vol. 51*, pp. 179–186, . DOI: https://doi.org/10.1016/j.conbuildmat.2013.10.054.

[18] A. Jansson, I. Löfgren, and K. Gylltoft, 2008. Design methods for fibre-reinforced concrete : A state-of-the-art review, Nord. Concr. Res., pp. 21–36.

[19] W. M. Souza, T. R. G. Caetano, M. P. Ferreira, and D. R. C. Oliveira, 2014. Shear strength of reinforced concrete one-way ribbed slabs, *IBRACON Struct. Mater. J., Vol. 7*(4), pp. 648–665. DOI: http://dx.doi.org/10.1590/S1983-41952014000400007.

Strength Performance of Sustainable Mortar Containing Recycle Sewage Sludge Ash (SSA)

Nurul Nazierah Mohd Yusri[1], Kartini Kamaruddin, Hamidah Mohd Saman, Nuraini Tutur

Faculty of Civil Engineering, Universiti Teknologi MARA
40450 Shah Alam, Selangor, Malaysia
[1]E-mail: nazierahoon@gmail.com

ABSTRACT

Sewage sludge is a by-product generated within the wastewater treatment process. Severe concern arised as the sludge are massively been dumped to the landfill and it may affect the environment. Many studies had been conducted in reusing the sewage sludge as construction material, where it is one of the optional ways to solve the issue. In this study, dried sewage sludge was incinerated with two different temperatures in order to produce sewage sludge ash (SSA), which are 800°C and 1000°C. After few processes, this SSA then reused in mortar as cement replacement with the replacement percentage of 5%, 10%, 15% and 20% by weight. The strength performance of mortar specimens was investigated after 7, 28, 60 and 90 days of curing. From the results, it is clearly showed that the compressive strength of all mortar specimens increased when the period of curing was prolonged. Moreover, almost all compressive strength of SSA mortars was higher than the control mortar. Therefore, there is potential to reuse this waste material as part of construction materials and hence, its plays an important role for future researches in minimisation of waste.

Keywords: *sewage sludge, sewage sludge ash, recycle, compressive strength, mortar*

INTRODUCTION

The problem regarding the waste generated had always been discussed globally since decades ago. This issue will be a crisis if a huge production of waste generated every day is not been taken care of. Wastewater from residential area, hospital, commercial, industrial establishments, and rain water are also considered as a waste [1]. The wastewater from the sewerage system is channelled to the wastewater treatment plant, where it will be treated with several processes before it can be released to the environment. At this point, the concern issue appears regarding the sewage sludge generated from the wastewater treatment process. Over the year, this semisolid by-product is massively being dumped into the landfill [2]. In Malaysia alone, it was reported that about 5.3 million m^3 sewage sludge was produced annually [3]. Without a proper disposal method, this might create various negative impacts to the environment. Hence, it is a vital to seek out an alternative root for the disposal method of sewage sludge, rather than be ended up at the landfill.

The global focus on sustainability and green technology approaches, somehow had affected the construction and cement industry. In 2013, it is reported that the world cement production had contributed roughly 9.5% of global CO_2 emission [4]. This justification had led to the numerous studies to search for the solution regarding this matter, which is part of it had shown an interest of reusing the waste or by-product as part of construction materials. It is fascinating that previous studies found that the sewage sludge had a potential to be reused in producing building and construction materials, as well as enhancing certain properties of conventional construction materials. The dried sewage sludge and sewage sludge ash (SSA) had been investigated to produce brick [5-6], lightweight aggregates [7-8], paver block [9], tiles [10], as cement substitution material for mortar and concrete [11-13], also as raw materials in cement blended production [14].

From the literatures, there were ranges of temperature used in incineration process from 550°C to 1200°C, in order to convert the dried sewage sludge into ashes form [11-15]. Tantawy *et al.* [1] stated that by using 800°C, it will help to preserve the pozzolanic value of the SSA, while finding by Tay and Show [16], showed that using SSA incinerated at 1000°C

had given the highest strength of mortar at 28 days of curing. As significant findings found through the literatures, this present study had been initiated to investigate the potential of local sewage sludge to be used as partial cement replacement in making mortar. Two temperatures to calcine the sludge, 800°C and 1000°C were adopted in the incineration process to form SSA.

METHODOLOGY

Preparation of Materials

Sewage sludge cake was collected from Indah Water (IWK) wastewater treatment plant at KLIA Sepang, Malaysia. The sewage sludge cake was then dried under the hot sun during the day time for about three to five days. This process needed in order to remove 70% to 90% of its moisture content. The dried sewage sludge then underwent controlled incineration to obtain the ashes and also to remove the organic matter content. Gas kiln furnace was used to conduct this incineration process, with temperature of 800°C and 1000°C; and it is burned for five hours. To get more fine powder of SSA, Ball Mill (Two Tier Jar) was used to ground sewage sludge ash (SSA) with 30 rpm for eight hours. All these processes are as shown in Figure 1. Figure 2 shows the particle of SSA after incineration and grinding process. XRF PANalytical was used to carry out the chemical composition analyses of SSA. Mining sand with the fineness modulus of 3.45 was used in this study. The grading of the fine aggregate was conducted according to ASTM C144-11 with sieve size between 0.063 mm to 5 mm. Type I Portland cement locally made was used in this present study.

The mix proportion ratio of 1:3 was used in this study, where it indicates one portion of cement was mixed with three portions of fine aggregate. The water cement ratio is taken as 0.5. For each temperature burning of SSA (800°C and 1000°C), four batches of SSA mortar mix with different percentages of SSA replacing cement were prepared. The percentages of SSA replacing cement by weight are 5%, 10%, 15% and 20%. These mortar specimens were cast in 50 mm x 50 mm x 50 mm cube mortar moulds. Without adding any SSA in the mix proportion, one batch of normal mortar was prepared as control. All mortar specimens were demoulded after

24-hours of casting and cured under water curing condition. All specimens were tested for compressive strength at the age of 7, 28, 60 and 90 days.

Testing Specimen

Compressive strength test of hardened mortar was conducted according to ASTM C109-13 [17]. The loading pace rate of 0.9 kN/s was applied. The data obtained from the testing was recorded to the nearest 0.05 N/mm^2, while the average result was rounded off to the nearest 0.1 N/mm^2. The compressive strength was calculated as given in Equation (1).

$$fm = P/A \qquad (1)$$

where:

fm = compressive strength (MPa or N/mm^2)
P = total maximum load (N)
A = area of loaded surface (mm^2)

Sewage Sludge Cake   Drying Process

Grinding Process   Incineration Process
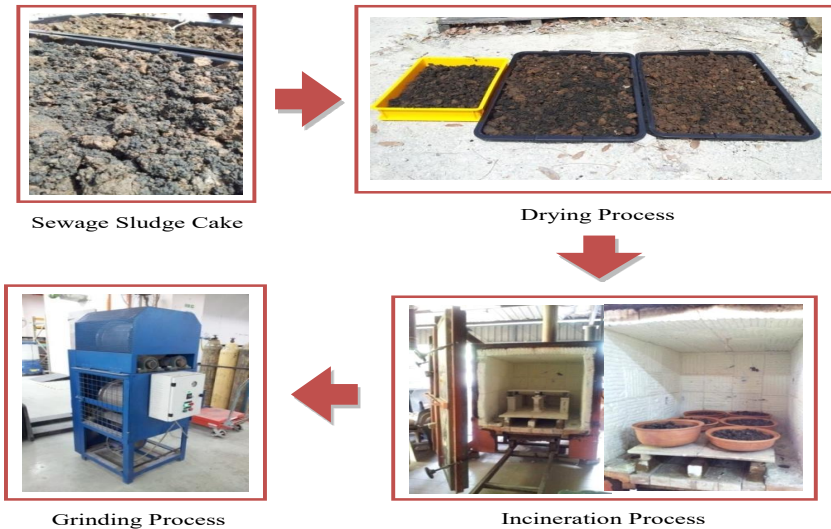
Figure 1: Processes to Convert the Sewage Sludge Cake to Sewage Sludge Ash (SSA)

a)   b)

Figure 2: a) Sewage Sludge Ash After Incineration Process; and b) Fine Sewage Sludge Ash (SSA) After Grinding Process

RESULTS AND DISCUSSION

Chemical Composition

The results from the XRF analysis are shown in Table 1. It presents the chemical composition of SSA incinerated at the temperature of 800°C and 1000°C, as compared to the Portland cement. Monzó *et al.* [18], enlighten that the chemical properties of sewage sludge differ from one another, depending on the origin of the wastewater and also the process conducted within the treatment plant. It is clearly shown that the four major compounds in both types of SSA (SiO_2, $Al2O_3$, $Fe2O_3$ and CaO), were also detected same as in the Portland cement. It was noticed that the SiO_2 and CaO oxides that found in the SSA affect the strength of mortar specimens [14]. Both SSA can be classified as Class C pozzolan material since it satisfies the standard requirement stipulated in ASTM C618-12a [19]. Therefore, these SSAs have the potential to be used as partial replacement for Portland cement in making mortar.

Table 1: Chemical Composition of Portland Cement, SSA Calcinated at 800°C and 1000°C (Mass in %)

Composition	Portland Cement	SSA 800˚C	SSA 1000˚C
SiO_2	14.2	34.2	35.3
$Al2O_3$	3.16	18.4	19.3
$Fe2O_3$	3.30	7.36	7.56
CaO	55.8	4.17	4.10
MgO	0.99	1.62	1.72
Na_2O	0.11	0.26	0.32
K_2O	0.53	2.08	2.15
Na_2O	0.11	0.26	0.32
K_2O	0.53	2.08	2.15
P_2O_5	0.04	8.97	9.31
SO_3	4.03	3.64	3.31
TiO_2	0.16	0.83	-
Others	0.33	0.65	-

Compressive Strength

Figure 3 demonstrates the compressive strength of SSA mortar (SSA incinerated at 800°C) and control mortar at the age of 7, 28, 60 and 90 days. It is clearly shown that all the mortar specimens experienced an increase in strength with respect to the increment of curing ages. At day 7 of age, nearly all the SSA mortar specimens exhibit highes compressive strength coressponding to control specimen which is 48.85 MPa, 49.91 MPa, and 43.64 MPa for those taht contained 5%, 10% and 20% replacement level of SSA (incinerated at 800ºC) respectively. While for the SSA800 15%, the compressive strength recorded is 41.07MPa, where it is slightly lower as compared to the normal specimens which recorded 42.38 MPa. However, as the age of curing increases, all SSA mortar specimens showed significant increase in compressive strength and it is much higher as compared to the normal mortar specimen. This can verify that the presence of SSA may assist the hydration process within the hardened specimens which had enhanced the strength development of the specimens at the longer hydration time.

Within the limited study, it was found that the compressive strength of mortarmade of SSA incinerated at 800°C, exceeded of control mortar. The mortar with 15% of replacement recorded higher compressive strength at 90 days of age, which marked 75.68 MPa. It was noted that the SSA mortar specimen with 5% and 15% replacement showed high strength among all.
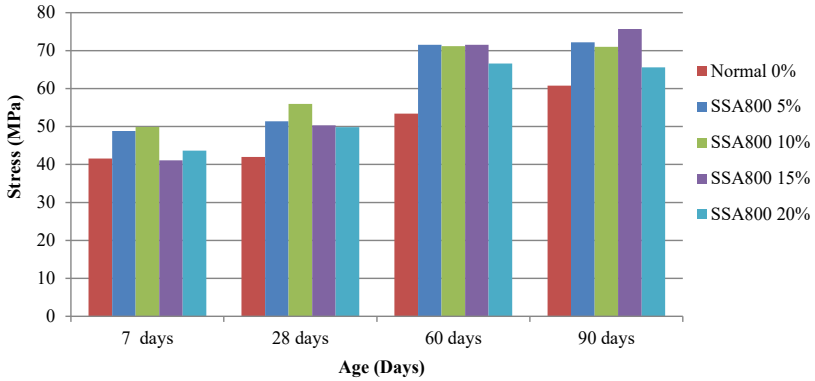
Figure 3: Compressive Strength of SSA Mortar which the Sludge was Incinerated at 800°C
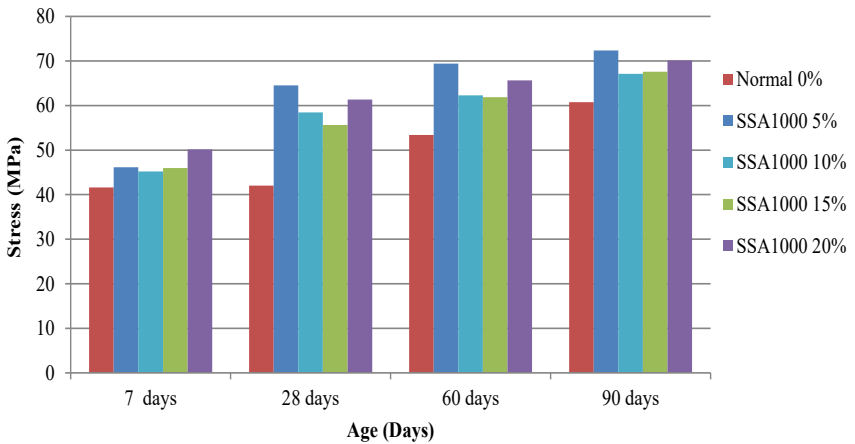
Figure 4: Compressive Strength of SSA Mortar which the Sludge was Incinerated at 1000°C

The compressive strength of SSA mortar which the sludge was incinerated at 1000°C compared to control mortar at the age of 7, 28, 60 and 90 days, is illustrated in Figure 4. The results showed that all SSA mortar specimens increased in compressive strength as compared with that of control mortar. The SSA mortar with 5% and 20% replacement level of SSA, showed a good strength development as the age of curing increased. Respectively, the compressive strength for SSA mortars at 90 days are 72.35 MPa for those containing 5% (SSA1000 5%), and 70.13 MPa for those containing 10% (SSA1000 20%) which are the highest strength achieved as compared to other series of mortar specimens. From this result, it is suggested that the SSA obtained from the incineration at 1000°C can partially replaced cement up to 20% to enhance the strength of mortar.
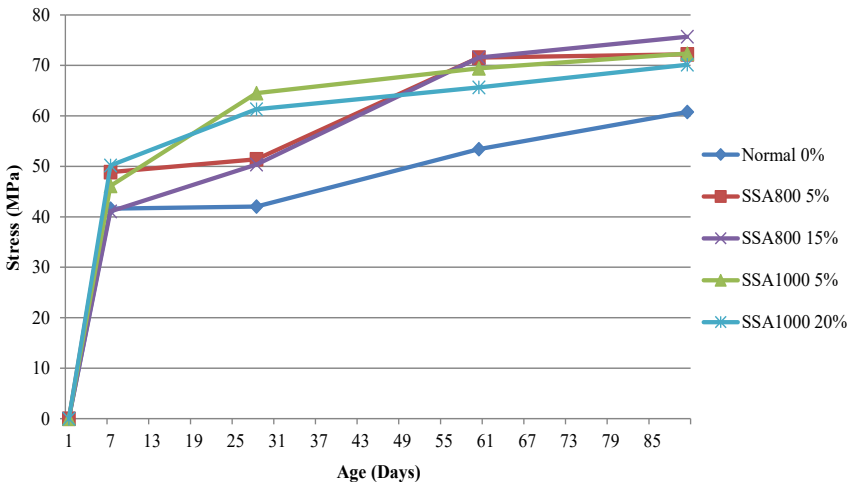
Figure 5: Compressive Strength of SSA Mortar Specimen with Respect to Two Different Incineration Temperatures

The compressive strength of SSA mortar with respect to incineration temperatures of 800°C and 1000ºC, which designated as SSA800 5%, SSA800 15%, SSA1000 5% and SSA1000 20% are demonstrated in Figure 5. It shows that all the SSA specimens developed its strength as the curing days prolonged. The higher strength development occurred in the earlier stage of curing, and it starts to slow down after 60 days of age, ascribed to the higher amount of SiO_2 and CaO content in SSA.

Interesting to note that all SSA mortar specimens (both incinerated at 800°C and 1000°C) exhibited higher compressive strength corresponding to the control mortar with respect to age of curing. These findings also claimed by Tay *et al.* [14], which had proved that SSA could enhance the mortar properties and belief that other than chemical composition content, the temperature and duration used during the incineration process, may influence in producing good quality of SSA. Therefore, this finding verified that SSA which incinerated at temperature of 800°C and 1000°C, have potential to be used as partial cement replacement material in making mortar.

CONCLUSION

From discussion of the present study, the findings are outlined as follows:
a.   Utilisation of SSA (produced by incineration temperature of 800°C and 1000°C) as cement replacement material in mortar mix, enhanced the compressive strength of the resulted SSA mortar.
b.   The optimum SSA as cement replacement material can be as high as 20% replacement by weight of cement in mortar making.
c.   Mortar that made of SSA incinerated at 800°C and replaced for 15% of cement attained the highest compressive strength.

It is suggested that this local made SSA has potential to be used as partial cement replacement material in making concrete or any reinforced concrete structure, such as wall panel, beam, slab etc. Further researches on long-term behaviour of SSA concrete need to be conducted before it is being practically used.

ACKNOWLEDGEMENT

REFERENCES

[1]   M. A., Tantawy, A. M., El-Roudi, E. M., Abdalla, and M. A., Abdelzaher, 2012. Evaluation of the pozzolanic activity of sewage sludge ash, *ISRN Chemical Engineering, Vol 12*, 1-8. DOI: http://dx.doi.org/10.5402/2012/487037.

[2]   J.H., Tay, and K.Y., Show, 1992. Utilization of municipal wastewater sludge as building and construction materials, *Resources, Conservation and Recycling Journal, Vol. 6*(3), pp. 191-204. DOI: https://doi.org/10.1016/0921-3449(92)90030-6.

[3]   M. R. S., Salmiati, U., Zaini,. and A., Shamila, 2012. Potential of sewage sludge as soil amendment. In *2nd International Conference on Environment and Industrial Innovation*, pp. 66-69.

[4]   G. J. O., Jos, J-M., Greet, M., Marilena, and A. H. W. P., Jereon, 2014. Trends in Global CO_2 Emission: 2014 Report. PBL Netherlands Environmental Assessment Agency.

[5]   K. Y., Chiang, P. H., Chou, C. R., Hua, K. L., Chien, and C., Cheeseman, 2009. Lightweight bricks manufactured from water treatment sludge and rice husks, *Journal of Hazardous Materials, Vol. 171*(1-3), pp. 76-82. DOI: https://doi.org/10.1016/j.jhazmat.2009.05.144.

[6]   J.H., Tay, 1987. Bricks manufactured from sludge, *Journal of Environmental Engineering, Vol. 113*(2), pp. 278-284. DOI: 10.1061/(ASCE)0733-9372(1987)113:2(278).

[7] J. I. Bhatty, and K. J., Reid, 1989. Moderate strength concrete from lightweight sludge ash aggregates, *The International Journal of Cement Composites and Lightweight Concrete, Vol. 11*(3), pp. 179-187. DOI: https://doi.org/10.1016/0262-5075(89)90091-2.

[8] Chesseman, C. R. and Virdi, G. S., 2005. Properties and microstructure of lightweight aggregate produced from sintered sewage sludge ash, *Resources, Conservation and Recycling Journal. Vol. 45*(1), pp. 18-30. DOI: 10.1016/j.resconrec.2004.12.006.

[9] K. K., Vijaya, 2012. Utilisation of sludge concrete in paver blocks, *International Journal of Emerging Trends in Engineering and Development, Vol. 4*(2), pp. 509-516.

[10] D. F., Lin, H. L., Luo, and S. W., Zhang, 2007. Effect of Nano-SiO2 on tiles manufactured with clay and incinerated sewage sludge ash, *Journal of Materials in Civil Engineering, Vol. 19*(10), pp. 801-808. DOI: https://doi.org/10.1061/(ASCE)0899-1561(2007)19:10(801).

[11] P., Garcés, M. P., Carrión, E., García-Alcocel, J., Payá, J. Monzó, and M. V., Borrachero, 2008. Mechanical and physical properties of cement blended with sewage sludge ash, *Waste Management Journal, Vol. 28*(12), pp. 2495-2502. DOI: 10.1016/j.wasman.2008.02.019.

[12] J., Monzó, J., Payá, M. V. Borrachero, and A., Córcoles, 1996. Use of sewage sludge ash (SSA) – Cement admixtures in mortars, *Cement and Concrete Research Journal, Vol. 26*(9), pp. 1389-1398. DOI: https://doi.org/10.1016/0008-8846(96)00119-6.

[13] S. C., Pan, D. H., Tseng, C. C., Lee, and C., Lee, 2003. Influence of fineness of sewage sludge ash on the mortar properties, *Cement and Concrete Research Journal, Vol. 33*(11), pp. 1749-1754.

[14] J.H., Tay, and K.Y., Show, 1994. Municipal wastewater sludge as cementitious and blended cement materials, *Cement & Concrete Composite Journal, Vol. 16*, pp. 39-48.

[15] C.M.A, Fontes, M. C., Barbosa, R. D. T., Filho, and J. P., Goncalves, 2004. Potential of sewage sludge ash as mineral additive in cement mortar and high-performance concrete. In I*nternational RILEm Conference on Use of Recycled Materials in Buildings and Structures*, Barcelona, Spain.8-11 November 2004, 797-806.

[16] J.H., Tay, and K.Y., Show, 1991. Properties of cement made from sludge, *Journal of Environmental Engineering, Vol. 117*(2), pp. 236-246. DOI: 10.1061/(ASCE)0733-9372(1991)117:2(236).

[17] American Society for Testing and Material. ASTM C109-13. Compressive Strength of Hydraulic Cement Mortars. ASTM International, West Conshohocken, Pa.

[18] J., Monzó, J., Payá, M. V. Borrachero, and I., Girbés, 2003. Reuse of sewage sludge ashes (SSA) in cement mixtures: The effect of SSA on the workability of cement mortar, *Waste Management Journal, Vol. 23*(4), pp. 373-381. DOI: 10.1016/S0956-053X(03)00034-5.

[19] American Society for Testing and Material. ASTM C618-12a. Standard Specification for Coal Fly Ash and Raw or Calcined Natural Pozzolan for Use in Concrete. ASTM International, West Conshohocken, Pa, 2012. DOI: 10.1520/C0618-12A.

Pull-Out Performance of T-Stub End Plate Connected To Concrete Filled Thin-Walled Steel Tube (CFTST) using Lindapter Hollo-Bolts

Nazrul Azmi Ahmad Zamri[1], Clotilda Petrus, Azmi Ibrahim, Hanizah Ab Hamid

Faculty of Civil Engineering, Universiti Teknologi MARA (UiTM),
40450 Shah Alam, Selangor Darul Ehsan, Malaysia
[1]E-mail: nazrul_azmi@yahoo.com

ABSTRACT

The application of concrete filled steel tubes (CFSTs) as composite members has widely been used around the world and is becoming popular day by day for structural application especially in earthquake regions. This paper indicates that an experimental study was conducted to comprehend the behaviour of T-stub end plates connected to concrete filled thin-walled steel tube (CFTST) with different types of bolts and are subjected to pull-out load. The bolts used are normal type bolt M20 grade 8.8 and Lindapter Hollo-bolt HB16 and HB20. A series of 10 mm thick T-stub end plates were fastened to 2 mm CFTST of 200 mm x 200 mm in cross-section. All of the specimens were subjected to monotonic pull-out load until failure. Based on test results, the Lidapter Hollo-bolts showed better performance compare to normal bolts. The highest ultimate limit load for T-stub end plate fasten with Lindapter Hollo-bolt is four times higher than with normal bolt although all end plates show similar behaviour and failure mode patterns. It can be concluded that T-stub end plate with Lindapter Hollo-bolt shows a better performance in the service limit and ultimate limit states according to the regulations in the design codes.

Keywords: *CFTST, Steel beam, T-stub end plate, connection, Hollo-bolt*

INTRODUCTION

To date, the Construction Industry Development Board (CIDB) is intensively encouraging Malaysian construction industries to develop an advance method for the capacity and capability in construction industries by introducing the implementation of Industrialised Building System (IBS). IBS is a construction system in which some parts are manufactured in factories, then are positioned and assembled into a structure on or off site with little extra site works [1]. Concrete filled steel tube (CFST) is a composite structural member where the steel hollow tube is made in factory, assembled and then filled up with concrete at construction site.

The steel hollow tube is used as permanent formwork as well as reinforcement for the structure and the concrete filled inside the hollow section increase the load capacities. It prevents the steel hollow tube to inward buckling. A CFST column is a structural system with excellent characteristics structurally, economically as compared to other types of columns such as the traditional reinforced concrete columns and steel columns.

A CFST offers many structural benefits such as has high compressive strength and ductility, has excellent earthquake resistance, is able to reduce cost and duration for the construction. These advantages have been widely exploited and have led to the extensive use of CFSTs in civil engineering structures. Many developed countries and also earthquake prone countries such as the United States, China, Australia have done many researches and using the system in their structural practices.

The utilisation of thin walled steel tube filled with concrete allows an economical solution primarily for an axially loaded column. For economical purposes, a thin walled steel section is sufficient to carry the construction loading while relatively inexpensive concrete is used as the major component to carry the design loading [2]. Studies done by [3-5] on the structural behaviour of concrete filled thin-walled steel tubes (CFTST) have proven that the performance of the thin-walled steel columns can be improved by providing sufficient internal stiffeners. However in these studies, the structural behaviour of CFTST columns were done in isolation. In order to apply CFTST columns in construction, a feasible connection between the column and beam must be identified.

STEEL BEAM-COLUMN CONNECTIONS

The use of concrete-filled steel tube (CFST) columns has become increasingly popular for civil engineering structures in developed countries such as England, Japan, United States of America for high rise buildings, bridges and other structural applications due to excellent earthquake resistance, ductility and also high strength capacity [6-7]. Due to this fact, many researchers have came out with various research works in order to enhance the beam to CFST column connections such as combination of welding and cutting through the steel hollow tubes [8]. These also included study on the effect of the different types of blind bolts [9], the effect of stiffness, strength of the connection using different end plate types and thicknesses [10].

Researchers [8][11] conducted studies on different types of beam-column connections such as simple welded connection, diaphragm connection, extending the steel beam through the steel tube, added weldable bars on top and bottom of the simple welded connection. Some of the connections showed very outstanding performances in the moment resisting and inelastic cyclic behaviour while the others were not. The most outstanding is the steel beam extended through the steel tube. This connection exhibits stable strain-hardening behaviour, develops a full plastic hinge in the beam-column connection and it can be used in regions of high seismic risk. However, the use of these types of connections has not always been convenient in construction practice. Considerable work during erection is required, in addition to extensive welding and high tolerances required in detailing.

In 2012, Wang and Guo [10] conducted a study on the connections of steel beams and concrete filled thin-walled steel tubes. Their study focusedon the effect of connections of flush and extended end plates onto two (2) different thicknesses of the steel hollow tubes namely 1.5 mm and 3 mm using extended blind bolts. It was found that the extended end plate showed better result compare to the flush end plate. Other than that, the thicker steel tube has lower deformation and higher moment capacity compare to the thinner steel tubes. Moreover, there was no sign of bending or shear deformation of the bolts in the tests except for the concrete near the bolts in tension which showed crack.

In 2011, a group of researchers from the Steel Construction Institute (SCI) and the British Constructional Steelwork Association (BCSA) has published guidance that covers a range of steelwork connections. The guidance focuses on nominally pinned joints that primarily carry vertical shear and, as an accidental limit state, tying forces, designed in accordance with Eurocode 3 and it's UK National Annexes [12]. Figure 1 shows the main components of steel connections as given in the guidance publication. However, this guidance is mainly for open section (H-section or C-section) and hollow section column without any infilled concrete.
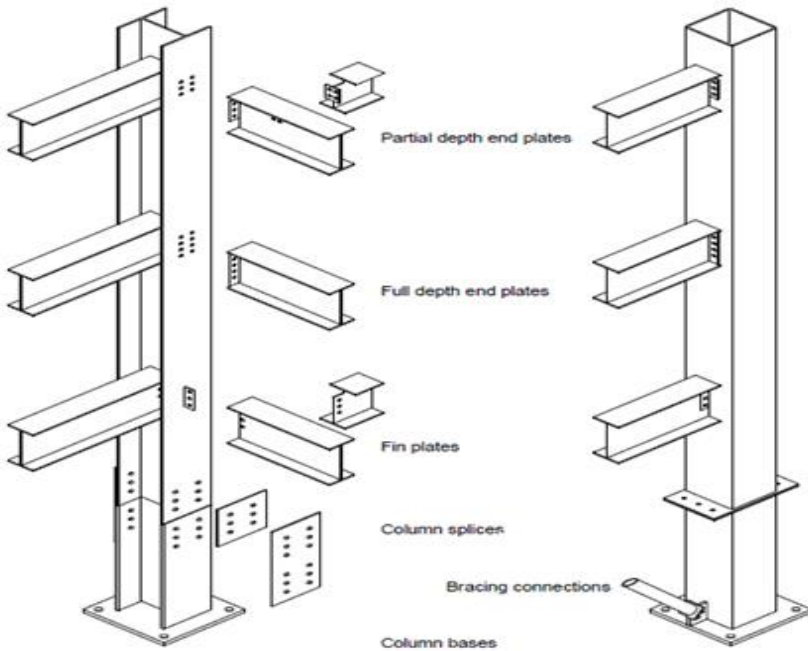
Figure 1: Typical Connections of Steel Column using Bolts [12]

From previous researches, it can be concluded that the usage of end plates shows a promising performance, however, the moment resistance of this connection is still lower compare to the beam through the steel tube connection. Moreover, the design guidance provided is still lacking especially for thin-walled section and also filled section. Thus, in order to fill this gap, a series of investigation has been carried out on T-stub end plate connected to concrete filled thin-walled steel tube (CFTST) with different types of bolts.

EXPERIMENTAL WORK

For this study, a laboratory work had been done where the T-stub end plate connecting to the skin of CFTST with two different types of bolts. A total of six specimens were prepared and tested. Two specimens were using normal bolts, whereas the other four were using Lindapter Hollo-bolts. Table 1 shows the summarised parameters for each specimen for this study. The size of square hollow section (SHS) for the CFST is 200 mm × 200 mm, the thickness is 2 mm and total length is 1200 mm. The SHS was fabricated from four (4) pieces of cold formed lipped angles that were seam weld to form a SHS with longitudinal stiffeners. The height of each longitudinal stiffener is 25 mm. Figure 2 shows how the sequence of SHS was fabricated.

Table 1: Parameters of Bolts for All Specimens

Specimen	Type of Bolt	Bolt Size (mm)	Bolt Lenght (mm)	Bolt Grade
B20-1	Normal bolt	20	90	8.8
B20-2	Normal bolt	20	120	8.8
HB20-1	Hollo-bolt	20	90	8.8
HB20-2	Hollo-bolt	20	120	8.8
HB16-1	Hollo-bolt	16	75	8.8
HB16-2	Hollo-bolt	16	100	8.8
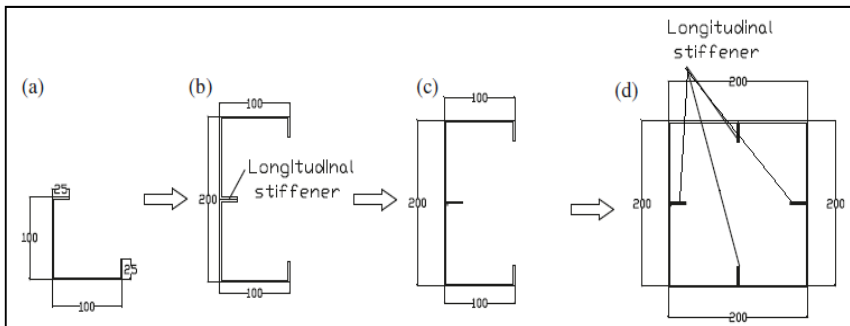
Figure 2: The Formation of the Steel Hollow Tube with Stiffeners (source by author)

M20 grade 8.8 normal bolts, HB16 and HB20 Lindapter Hollo-bolts were used to connect the T-stub to the CFTST skin. Additional parameter which is the different length of the each bolt had also been observed. Figure 3 and 4 show the dimensions and components of the Lindapter Hollo-bolt respectively.
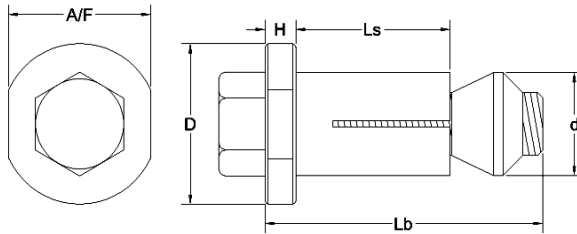
Bolt type	Bolt diameter, d_b (mm)	Bolt length, L_b (mm)	Sleeve length, L_s (mm)	Sleeve diameter, d (mm)	Collar Thickness, H (mm)	Collar Thickness, D (mm)	Collar Across flat, A/F (mm)
HB16-1	16	75	41.5	25.75	8	38	36
HB16-2	16	100	41.5	25.75	8	38	36
HB20-1	20	90	50	32.75	10	51	46
HB20-2	20	120	50	32.75	10	51	46

Figure 3: Dimensions of Hollo-Bolt Components (source by author)
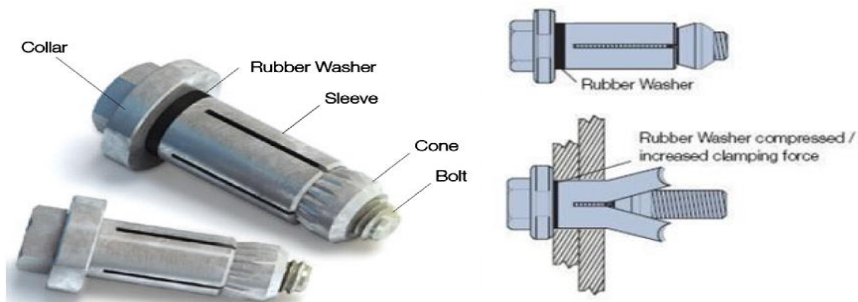
Figure 4: Components of Lindapter Hollo-Bolt [13]

The dimensions of the T-stub end plate and steel hollow section are consistent for all specimens. The dimensions of steel sections and bolt locations are shown in Figure 5.
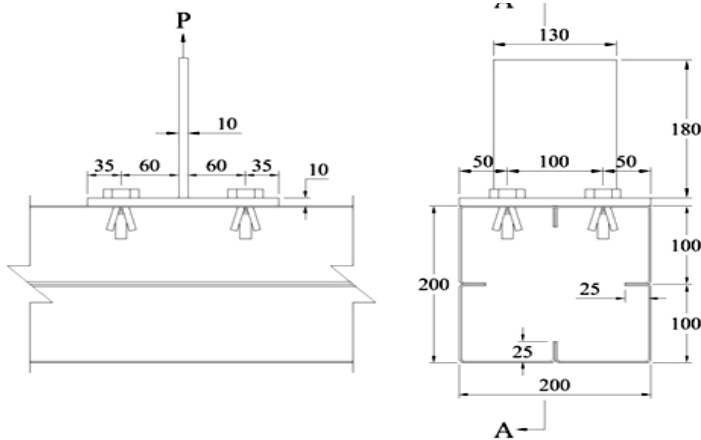
Figure 5: The Arrangement of Hollo-Bolt and T-Stub End Plate (All Dimensions are in mm) (source by author)

The installation for the T-stub end plate is different for the normal bolts compare to Lindapter Hollo-bolts. To fasten normal bolts, both sides of the bolts which are inside and outside of the steel hollow section need to be reachable and secure. It is proven that this method is not very suitable for onsite practices. Different to normal bolts, Lindapter Hollo-bolts can be fasten from outside of the hollow section only. Figure 6 shows installation steps for Hollo-bolts.
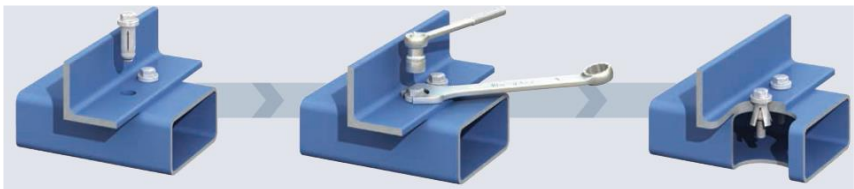
Figure 6: Installation of Hollo-Bolt [13]

Figure 7: Completed Assemblage of T-Stub End Plate to the CFST using Hollo-Bolt (source by author)

| (a) | (b) |

Figure 8: Different Setting of (a) Hollo-Bolt and (b) Normal Bolt After Installation (source by author)

Figure 7 show the assemblage of T-stub end plate to the CFST column with Hollo-bolts, while Figure 8 shows differences between normal bolts and Hollo-bolts installation setting inside the steel hollow tubes. Compare to normal bolts, the Hollo-bolts sleeve can improve the bonding between the bolts and concrete. Figure 9 and Figure 10 show the support setup of CFST and T-stub end plate respectively for the pull-out test. The specimens were tested until failure under monotonic load. All data and behaviour of the specimens were recorded and observed.

Figure 9: Overall Setup for the Pull-Out Experiment (source by author)

Figure 10: The T-Stump End Plate Setting for the Test (source by author)

RESULTS AND DISCUSSION

The concrete used for this experiment was designed for grade C30 and the tensile strength for the steel sections are 403 MPa and 330 MPa for 2 mm and 10 mm steel plate respectively. The concrete strength for each specimen was different because each concrete batch has to be mixed at different times due to lack of concrete mixer capacity for each mix. Therefore, the results shown had been normalised according to the concrete strength for each specimen.
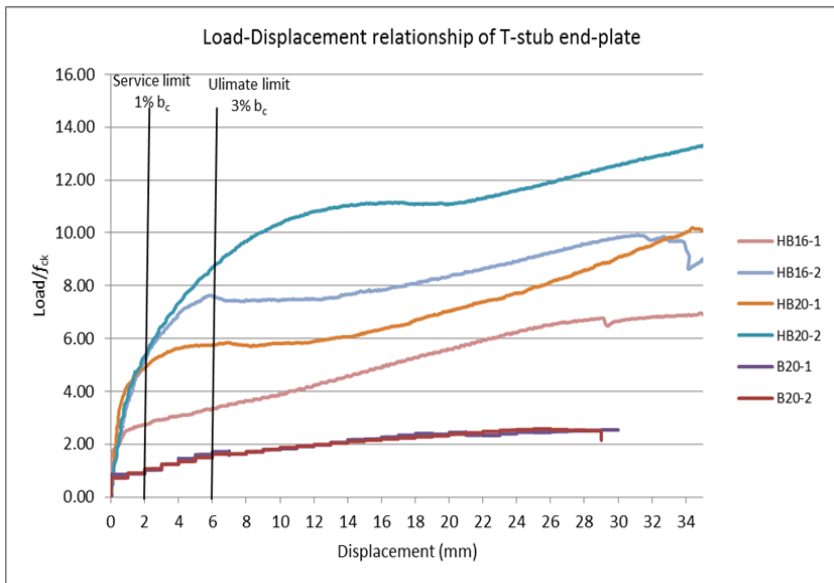
Figure 11: The Load-Displacement Behaviour of the Specimens (source by author)

The load-displacement relationship curves of the specimens were plotted and are shown in Figure 10. Each load was plotted against a transducer at mid-point of the end plate where the displacement at this point is most critical. From the graph, the specimens with normal bolts do not contribute much even though different lengths of the bolts were used. The specimens with Hollo-bolts showed better performance where they resisted higher loads compare to the normal bolts.

International Institute of Welding, IIW [14] and [15] recommended that the T-stub should be designed to transfer a limited amount of tension force in order to ensure that the column face deformation will not exceed serviceability limit state at 1% of the column width and will be no more than ultimate limit state at 3% of the column width where in this study serviceability and ultimate limit state are at 2 mm and 6 mm, respectively.

The graphs in Figure 11 indicate that T-stub end plates connected with normal bolts have the lowest value of load for both service and ultimate limit states. By using Hollo-bolts, there is huge increase in loads for both limit states. Even though the load factor for ultimate limit state for HB16-2, HB20-1 and HB20-2 are different, the load values for service limit state are almost the same at 5.0 kN/fck.
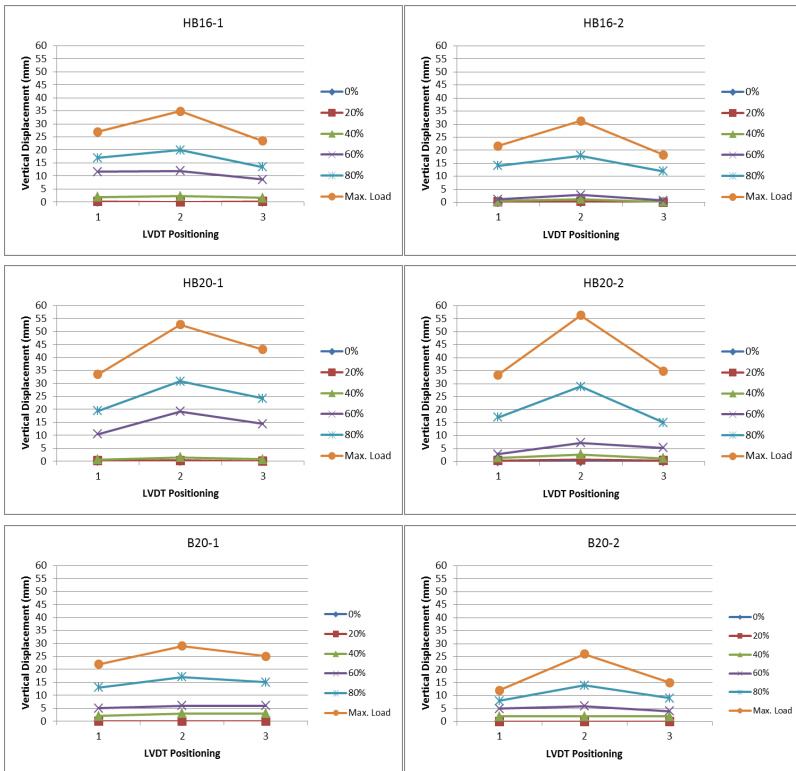
Figure 12: The Vertical Deformation of the T-Stub End Plate (source by author)

All specimens showed similar behaviour and failure modes at the end of the test. All specimens' end-plates yielded at the flange plates and caused the end-plates to bend vertically upward before the bolts reached their yield point. Figure 12 shows the deformations of the T-stub end-plates before they reach their maximum loads during the test. Figure 13 shows the actual deformation of T-stub end plates for both types of bolts.

Other than the deformation of the end plates, the column faces of CFTST experienced punching failure and buckled outward due to the pull-out. In this experiment, the expanded sleeve of the Hollo-bolts did contribute largely to the performance because it gave more surface contact area between the bolts and concrete. At the end of the test, the bolts for all specimens were removed and are shown in Figure 13. HB16-1 and HB16-2 bolts show similar behaviour where all bolts bent at the contact area between the end plate and concrete core as in Figure 14(a). However, HB20-1, HB20-2, B20-1 and B20-2 did not deform and damage as much as the other bolts as shown in Figure 14(b).

Figure 13: The Failure Modes of The Specimens (source by author)

(a)   **(b)**

Figure 14: Deformation of Bolts After Test (source by author)

CONCLUSION

Currently, it can be concluded that the T-stub end plates with Lindapter Hollo-bolts showed better performance compare to the plates with normal bolts both, in terms of service and ultimate limit states, and deformation of the end plates. The lengths of bolts also give different outcome especially for Hollo-bolts because their sleeves were designed according to the length of the bolts. The longer bolt performed better in both limit states and the deformation of end plates. As for the design limit states, HB16-2, HB20-1 and HB20-2 perfomed equally good at service limit state but performed differently at ultimate limit state.

RECOMMENDATION

In this study, the test was restricted to the difference between having either normal bolts or Lindapter Hollo-bolts with constant end plate size for all specimens. There are other types of blind bolts and rivets such as Ajax blind bolt and flowdrill that can also be used as fasteners. By using these types of bolts instead with CFTST, it may give various outcomes that can be looked intofor a better understanding of thin walled structure connections.

ACKNOWLEDGEMENT

REFERENCES

[1] Industrialized Building System (IBS) Road Map (2003 – 2010), 2003, Lembaga Pembangunan Industri Pembinaan Malaysia (CIDB). Malaysia.

[2] M. Mursi, and B. Uy, 2004. Strength of slender concrete filled high strength steel box columns, *Journal of Constructional Steel Research, Vol. 60*(12), pp. 1825-1848. DOI: https://doi.org/10.1016/j.jcsr.2004.05.002.

[3] Z. Tao, L.H., Han, and Z.B., Wang, 2005. Experimental behaviour of stiffened concrete-filled thin-walled hollow steel structural (HSS) stub columns, *Journal of Constructional Steel Research, Vol. 61*(7), pp. 962–983. DOI: https://doi.org/10.1016/j.jcsr.2004.12.003.

[4] C. Petrus, A. H. Hanizah, I. Azmi and G. Parke, 2010. Experimental behaviour of concrete filled thin walled steel tubes with tab stiffeners, *Journal of Constructional Steel Research, Vol. 66*(7), pp. 915-922. DOI: https://doi.org/10.1016/j.jcsr.2010.02.006.

[5] C. Petrus, A. H. Hanizah, I. Azmi and D. N. Joe, 2011. Bond strength in concrete filled built -up steel tube columns with tab stiffeners, *Canadian Journal of Civil Engineering, Vol. 38*(6), pp. 627-637. DOI: https://doi.org/10.1139/l11-030.

[6]   A. Elremaily and A. Azizinamini, 2002. Behavior and strength of circular concrete-filled tube columns, *Journal of Constructional Steel Research. Vol. 58*(12), pp. 1567-1591. DOI: https://doi.org/10.1016/S0143-974X(02)00005-6.

[7]   K. Abedi, A. Ferdousi and H. Afshin, 2008. A novel steel section for concrete-filled tubular columns, *Thin-Walled Structure, Vol. 46*(3), pp. 310–319. DOI: https://doi.org/10.1016/j.tws.2007.07.019.

[8]   Y. M. Alostaz and S. P. Schneider, 1996. Analytical behavior of connections to concrete-filled steel tubes, *Journal of Constructional Steel Research. Vol. 40*(2), pp. 95–127. DOI: https://doi.org/10.1016/S0143-974X(96)00047-8.

[9]   A. P. Gardner and H. M. Goldsworthy, 2005. Experimental investigation of the stiffness of critical components in a moment-resisting composite connection, *Journal of Constructional Steel Research, Vol. 61*(5), pp. 709–726. DOI: https://doi.org/10.1016/j.jcsr.2004.11.004.

[10] J. F. Wang and S. P. Guo, 2012. Structural performance of blind bolted end plate joints to concrete-filled thin-walled steel tubular columns, *Thin-Walled Structures, Vol. 60*, pp. 54–68. DOI: https://doi.org/10.1016/j.tws.2012.07.006.

[11] S. P. Schneider and Y. M. Alostaz, 1998. Experimental behavior of connections to concrete-filled steel tubes, *Journal of Constructional Steel Research, Vol. 45*(3), pp. 321-352. DOI: https://doi.org/10.1016/S0143-974X(97)00071-0.

[12] E. N. Moreno, M. Banfi, D. Brown, M. Fewster, P. Gannon, C. Gibbons, B. Hairsine, A. Hughes, F., Kelly, A., Malik, D., Moore, C., Morris, D., Nethercot, A., Pillinger, S., Prestidge, A., Rathbone, R., Reed, C., Robinson, C., Robinson, G., Simmons, C., Colin Smart, B., Staley, M., Tiddy, and R., Weeden, 2011. *Joints in Steel Construction: Simple Joints to Eurocode 3 (P358)*, England: The Steel Construction Institute (SCI).

[13] Hollo-Bolt, 2013. The Original Expansion Bolt for Structural Steel, Lindapter, England.

[14] J., Lee, 2011. Blind Bolted Connections for Steel Hollow Section Columns in Low Rise Structures. Unpublished PhD's Thesis, Department of Civil and Environmental Engineering, University of Melbourne, Australia.

[15] International Institute of Welding (IIW), 1989. Design Recommendations for Hollow Section Joints – Predominantly Statically Loaded. 2nd ed. Helsinki, Finland.

The Application of Waste Marble as Coarse Aggregate in Concrete Production

Kok Yung Chang, Wai Hoe Kwan*, Hui Bun Kua

Department of Construction Management
Universiti Tunku Abdul Rahman (UTAR), Kampar Campus
Jalan Universiti, Bandar Baru, 31900 Kampar, Perak, Malaysia.
*E-mail: kwanwh@utar.edu.my

ABSTRACT

The massive growth of construction industry especially in the developing countries results in extensive quarrying activities which ultimately would lead to the depletion of natural resources. Apart from extensive extraction of the natural granite from the earth for concrete production, marble production industry is also majorly contributing to the quarrying activities. In addition, high volume of waste is generated by the marble production industry as 70% of marble is wasted during the production such as quarrying, cutting, processing and others which is environmental unfriendly. In a way to achieve sustainable construction, the present study is to utilise the waste marble in replacing the coarse aggregate in concrete production. The engineering performance including workability, compressive strength, ultrasonic pulse velocity (UPV) and chloride penetration were analysed. The raw waste marble obtained from the industry were crushed and sieved into maximum size 20 mm and used to replace the coarse aggregate at the level of 20%, 40%, 60%, 80% and 100% respectively. Results show that 60% of the replacement level has yield to optimum result by achieving the highest compressive strength and UPV at approximate 5% higher than the control. Meanwhile, the effect on chloride penetration resistance is more significant, i.e. approximate 19% better than the control. However, increasing the replacement level of waste marble has no significant effect on workability, although an increasing trend was observed.

Keywords: *waste marble, coarse aggregate replacement, concrete, environmental*

INTRODUCTION

Due to the continuous development, the quarrying activities are increasing to cater the demand of coarse aggregate for concrete production. Although the earth is rich in natural resources, the extensive and endlessly quarrying of coarse aggregate can cause depletion of available resources and ecological problems to the environment. Besides, marble production is not an environmental friendly activity. Approximately, 70% of marble were wasted during the production such as quarrying, processing and polishing [1]. Even though the waste marble is not hazardous, it destroys plants and causes pollution [2]. On the other hand, disposal of waste marble is not viable as it may reduce the permeability of soil and the fertility of soil will be affected as it increases its alkalinity [3]. Therefore, the aim of this study is to study the engineering performance of the crushed waste marble when use as coarse aggregate replacement in concrete production. This measure can be viewed as a sustainability measure as it reduces the solid waste disposal and slows down the pace of resources depletion.

Shirule *et al.* [4] and Vaidevi [5] reported that the replacement of cement with marble powder up to 10% by weight increase the compressive strength. Moreover, Aliabdo *et al.* [6] investigated in another study and found that 10% of cement replaced by marble dust enhances the mechanical properties of concrete. Nonetheless, the results show that 15% replacement of sand by marble dust is the optimum replacement level to provide the highest compressive strength. Another study reported by Corinaldesi *et al.* [7] shows that 10% replacement of fine sand by waste marble powder possessed higher compressive strength with similar workability properties. Hebhoub *et al.* [1] studied the use of waste marble aggregates as fine and coarse aggregate replacement materials in concrete. The study elucidates that the substitution of natural aggregates by waste marble is beneficial to the concrete performance. From the review on the current literatures, it is found that the majority of the studies are exploring on the effects of substituting the fine aggregate with waste marble. The crushed waste marble that acts as replacement material for coarse aggregate in concrete production is scarcely reported. Substituting the coarse aggregate could be more economically viable as the amount of energy and cost to spend on crushing the waste marble is greatly reduced.

EXPERIMENTAL PROGRAMME

In this study, the Portland composite cement manufactured by YTL Cement in accordance with BS EN 197-1:2000 [8] was used as the binder in concrete. Meanwhile, the filler part consist of natural granite as coarse aggregate and mining sand as fine aggregate in concrete. The waste marble was collected from Sri Martek Marble Industries Sdn. Bhd. in Perak, Malaysia. The waste marble was crushed to coarse aggregate size with not more than 20 mm. The crushed waste marble is shown in Figure 1 and the physical properties of the natural granite and crushed waste marble is shown in Table 1.

Figure 1: Crushed Waste Marble (source by author)

Table 1: Physical Properties of Coarse Aggregates Used

Physical Properties	Natural Granite	Crushed Waste Marble
Specific gravity	2.62	2.66
Fineness modulus	7.97	7.90
Average flakiness index (%)	18	13
Water absorption (%)	0.35	0.30
Moisture content (%)	0.15	0.05

In this study, conventional normal concrete was used as the control mixture and the replacement ratio of coarse aggregate is 20%, 40%, 60%, 80% and 100% while the water-to-cement (W/C) ratio was maintained at 0.4. The concrete mix design is summarised in Table 2. Several tests were carried out to assess engineering performance, including slump, compressive strength, ultrasonic pulse velocity, and chloride penetration. The slump test was performed in accordance with BS EN 12350-2 [9] while the compressive

strength of concrete was tested up to 90 days in accordance with BS EN 12390-4 [10]. The ultrasonic pulse velocity (UPV) was carried out in accordance with BS EN 12504-4 [11] while chloride penetration depth were performed according to the method used by Guneyisi, Ozturan and Gesoglu [12]. The specimens for chloride penetration test were cured in normal water for 28 days and then immersed in 4% sodium chloride solution until the testing age. At the testing age, the cube specimen was cut into half and the freshly cut surfaces were then sprayed with 0.1 N silver nitrate solution.

Table 2: Crushed Waste Marble Concrete Mix Design

Mix	Cement (kg/m3)	Fine Aggregate (kg/m³)	Natural Granite (kg/m³)	Crushed Waste Marble (kg/m³)	W/C ratio
CM	422	980	980	0	
M1	422	980	784	196	
M2	422	980	588	392	0.4
M3	422	980	392	588	
M4	422	980	196	784	
M5	422	980	0	980	

RESULTS AND DISCUSSION

Slump Test

Figure 2 shows the workability of all concrete mixtures. The result shows that the replacement level of crushed waste marble has no significant effect on workability as all of them were still categorised as medium slump. Besides, it shows that the workability is slightly increasing with the replacement ratio of crushed waste marble but this is contradicted with other researches [13-14]. This could be probably due to different sources of marble were used. However, from the flakiness index and water absorption data in Table 1, the values of crushed waste marble were slightly lower than the natural granite in both properties. These would contribute to better workability properties in fresh concrete [15].
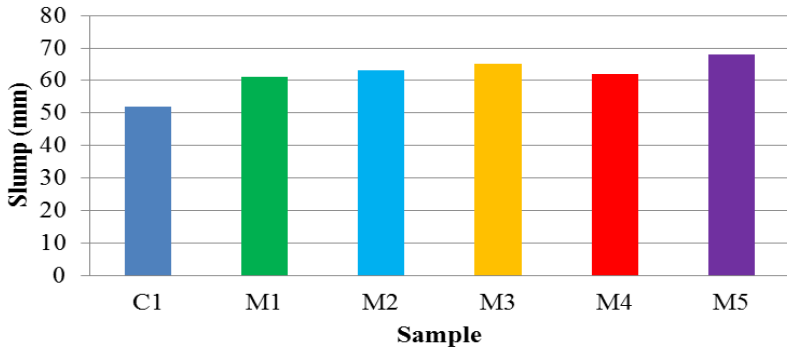
Figure 2: Slump Values of Various Specimen

Compressive Strength

The compressive strength of various concrete specimens was examined at 7, 14, 28 and 90 days. Figure 3 illustrates the strength development are similar in the control mixture (CM) and other mixtures containing crushed waste marble. This can be concluded that the replacement of crushed waste marble would not affect the strength development of concrete matrix. The result also shows concrete containing 60% crushed waste marble in the coarse aggregate (M3) obtained higher compressive than control mixture (CM). The recorded strength of the M3 at 90 days was 39.95 N/mm², approximate 5% higher than the control specimen. This could be explained that the more rounded crushed waste marble helped to create better particles formation in the concrete matrix and consequently it yields better bonding among the binder and filler which ultimately render a denser matrix [1].
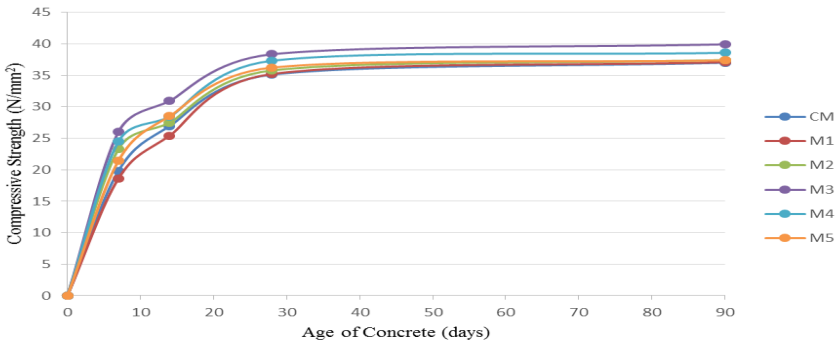
Figure 3: Compressive Strength of Specimens at Different Level of Marble Replacement

Ultrasonic Pulse Velocity (UPV)

Ultrasonic pulse velocity test is a non-destructive test that used for determination of the speed velocity of propagation of pulses of ultrasonic waves through hardened concrete. It can be used to determine the quality of the concrete in term of the amount of the voids or cracks presence in the concrete. The pulse velocities of concrete specimens are shown in Figure 4 and the results show that the concrete specimens' quality was excellent as the pulse velocities are above 4.5 km/h in accordance with the UPV assessment guidelines. Among all specimens, M3 is the best as it exhibits the highest value, i.e. 4.78 km/h. This is consistent with the compressive strength analysis where the M3 specimen has obtained the highest strength at all testing ages. Hence, it leads to a conclusion that M3 mix has produced better microstructure formation than the other specimens.

Figure 4: UPV Values of Various Specimen

Chloride Penetration Depth

The durability of the reinforced concrete depends on the capability of concrete cover to prevent the reinforcement from corrosion within the concrete. The corrosion of reinforcement in the concrete structure is the most common factors causing structure deterioration in the long term [12]. Hence, chloride penetration depth of the specimens was determined in this study. The chloride penetration depth was determined after immersion in 4% sodium chloride solution for 7, 14 and 28 days. M3 has the lowest chloride penetration depth at 28 days, i.e. 12.6 mm at approximate 19% lower than that of the control specimen. The better resistance against the chloride penetration could be due to better microstructure formation. Neville [15] explains that higher compressive strength is a result of lower porosity in the concrete matrix and this was also justified in the UPV test.

Table 4: Average Chloride Penetration Depth

Specimen	Average Chloride Penetration Depth (mm)		
	7 days	14 days	28 days
CM	9.6	11.4	15.5
M1	9.1	11.8	14.8
M2	9.0	11.4	15.6
M3	8.7	9.5	12.6
M4	9.3	11.4	15.2
M5	9.0	12.0	15.0

CONCLUSION

Based on the results and discussion, few conclusions are drawn as below:
i.   The workability of concrete was not affected by the replacement of crushed waste marble and it gave slightly higher workability than normal concrete.
ii.   The optimum mixture is the concrete with 60% replacement of crushed waste marble (M3) as it has the highest compressive strength compared to the other concrete mixes. Besides that, the strength development trend is in line with the conventional concrete.

iii. The quality of concrete specimens was excellent as the UPV values were above 4.5 km/h. Besides, M3 has the highest value which is 4.77 km/h, which indicates that it has lesser amount of voids and micro cracks.

iv. The concrete with 60% replacement of crushed waste marble (M3) has highest resistance against the chloride penetration as the penetration depth was 12.6 mm.

REFERENCES

[1] H. Hebhoub, H. Aoun, M. Belachia, H. Houari and E. Ghorbel, 2011. Use of waste marble mggregates in concrete, *Construction and Building Materials, Vol. 25*(3), pp. 1167-1171. DOI: https://doi.org/10.1016/j.conbuildmat.2010.09.037.

[2] R.A. Hamza, S. El-Haggar and S. Khedr, 2011. Marble and granite waste: Characterization and utilization in concrete bricks, *International Journal of Bioscience, Biochemistry and Bioinformatics, Vol. 1*(4), pp 286-291. DOI: 10.7763/IJBBB.2011.V1.54.

[3] A. Awol, 2011. Using marble waste powder in cement and concrete production. Unpublished PhD thesis, Addis Ababa University, Ethiopia.

[4] P.A. Shirule, A. Rahman and R.D. Gupta, 2012. Partial replacement of cement with marble dust powder, *International Journal of Advanced Engineering Research and Study, Vol. 1*(3), pp 175-177.

[5] C. Vaidevi, 2013. Study on marble dust as partial replacement of cement in concrete, *India Journal of Engineering, Vol. 4*(9), pp 14-16.

[6] A.A. Aliabdo, A.E.M.A., Elmoaty and E.M. Auda, 2014. Re-use of waste marble dust in the production of cement and concrete, *Construction and Building Materials, Vol. 50*, pp 28–41. DOI: https://doi.org/10.1016/j.conbuildmat.2013.09.005.

[7]   V. Corinaldesi, G.G. Moriconi and R.N. Tarun, 2010. Characterization of marble powder for its use in mortar and concrete, *Construction and Building Materials, Vol. 24*(1), pp 113-117. DOI: https://doi.org/10.1016/j.conbuildmat.2009.08.013.

[8]   BS EN 197-1. 2000. Cement Composition, Specifications and Conformity Criteria for Common Cements. British Standard Institution.

[9]   BS EN 12350-2. 2009. Testing Fresh Concrete: Slump Test. British Standard Institution.

[10]   BS EN 12390-4. 2000. Testing Hardened Concrete. Compressive Strength. Specification for Testing Machines. British Standard Institution.

[11]   BS EN 12504-4. 2004. Testing Concrete. Determination of Ultrasonic Pulse Velocity. British Standard Institution.

[12]   E. Guneyisi, T. Ozturan and M. Gesoglu, 2007. Effect of initial curing on chloride ingress and corrosion resistance characteristics of concrete made with plain and blended cements, *Building and Environment, Vol. 42*(7), pp 2676-2685. DOI: 10.1016/j.buildenv.2006.07.008.

[13]   F.J.F. Gameiro, 2013. Durability Properties of Structural Concrete incorporating Fine Aggregates from the Waste Marble Industry, Extended Abstract, pp 1-14.

[14]   D. Silva, F. Gameiro and J. Brito, 2014. Mechanical properties of structural concrete containing fine aggregates from waste generated by the marble quarrying industry, *Journal of Materials in Civil Engineering, Vol. 26*(6), pp 1-8. DOI: https://doi.org/10.1061/(ASCE)MT.1943-5533.0000948.

[15]   A.M. Neville, 1995. *Properties of Concrete, 4th ed*. Edinburgh Gate: Person Education Limited.

GUIDELINES FOR SUBMISSION OF ARTICLES

The Scientific Research Journal (SRJ) (ISSN: 1675-7009) is an international refereed journal, jointly published by the Institute of Research Management and Innovation (IRMI) and the UiTM Press, Universiti Teknologi MARA (UiTM), Malaysia. This journal was launched in the hope of stimulating quality research projects in science and technology related areas. Researchers are strongly encouraged to use this journal as a platform for publishing and disseminating their research findings to the members of academia and the community at large.

The SRJ publishes research papers that address significant issues in the fields of science and technology including life science, natural science, health science and physical science. It provides a balanced presentation of articles and solicits contributions from the fields of: Engineering, Computer Science, Mathematical Sciences, Energy, Environmental Science, Materials Science, Physics, Chemistry, Astronomy, Pharmacy, Medicine and Applied Sciences.

Emphasis is place on direct and clearly understood communication, originality and scholarly merit. Only original papers will be accepted and copyright of published papers will be vested in the publisher.

Submitted manuscripts should be written in English with production-quality figures. Manuscripts should be typed using Times New Roman (point 12), single-line spacing and wide margins (2.54 cm left, right, top and bottom). The manuscript should include the title of the paper; the name, address, contact numbers and email(s) of the correspondence author; a short abstract of between 200 and 300 words, which clearly summaries the paper with 4-5 keywords. Submission should be limited to a maximum of 20 typed pages.

Tables should be included within the text where appropriate and must be numbered consecutively with Arabic numerals and have titles that precede the table. Similarly, all figures must be numbered and a detailed caption should be provided below each figure. Figures should be embedded within the text where appropriate. Glossy photographs when required

should be scanned to a suitable resolution (1200 dpi), which enables quality reproduction.

References should be numbered in ascending order and cited within square brackets, e.g. [1], [3-5], in the main body of the text. References included at the end of the manuscript are to be in the order that they appear in the main body of text. Some entry samples are as follows:

[1]   A. B. Author, 2000. *Title of Book,* ABC Press, Kuala Lumpur, Malaysia.

[2]   C. D. Author and E. F. Author, 1999. Title of Paper, *Journal Name, Vol. 10*, pp. 32-45.

[3]   G. H. Author, 2006. Title of the conference paper, in Proceedings of the 2000 IEEE International Symposium on Circuits and Systems, Geneva, Switzerland, pp. 100-105

Manuscripts submitted to the journal will be initially screened by the Chief Editor, to determine appropriateness. Only those manuscripts considered of a sufficiently high standard will proceed to undergo a double blind review.

Upon completion, the manuscripts will be passed to an editorial board member for appraisal of their value. Additionally, they will be reviewed by an expert in that discipline.

For further information, please contact:
Professor Dr. Hamidah Mohd Saman
Chief Editor
Scientific Research Journal
Institute of Research Management and Innovation
Universiti Teknologi MARA
40450 Shah Alam Selangor,
MALAYSIA
E-mail: hamid929@salam.uitm.edu.my

Or e-mail SRJ's Secretariat: srj_editor@salam.uitm.edu.my/ khairul2950@ salam.uitm.edu.my